

# Altered Repolarization Reserve in Failing Rabbit Ventricular Myocytes

## Calcium and $\beta$ -Adrenergic Effects on Delayed- and Inward-Rectifier Potassium Currents

See Editorial by Fu and Laurita

**BACKGROUND:** Electrophysiological remodeling and increased susceptibility for cardiac arrhythmias are hallmarks of heart failure (HF). Ventricular action potential duration (APD) is typically prolonged in HF, with reduced repolarization reserve. However, underlying  $K^+$  current changes are often measured in nonphysiological conditions (voltage clamp, low pacing rates, cytosolic  $Ca^{2+}$  buffers).

**METHODS AND RESULTS:** We measured the major  $K^+$  currents ( $I_{Kr}$ ,  $I_{Ks}$ , and  $I_{K1}$ ) and their  $Ca^{2+}$ - and  $\beta$ -adrenergic dependence in rabbit ventricular myocytes in chronic pressure/volume overload-induced HF (versus age-matched controls). APD was significantly prolonged only at lower pacing rates (0.2–1 Hz) in HF under physiological ionic conditions and temperature. However, when cytosolic  $Ca^{2+}$  was buffered, APD prolongation in HF was also significant at higher pacing rates. Beat-to-beat variability of APD was also significantly increased in HF. Both  $I_{Kr}$  and  $I_{Ks}$  were significantly upregulated in HF under action potential clamp, but only when cytosolic  $Ca^{2+}$  was not buffered. CaMKII (Ca<sup>2+</sup>/calmodulin-dependent protein kinase II) inhibition abolished  $I_{Ks}$  upregulation in HF, but it did not affect  $I_{Kr}$ .  $I_{Ks}$  response to  $\beta$ -adrenergic stimulation was also significantly diminished in HF.  $I_{K1}$  was also decreased in HF regardless of  $Ca^{2+}$  buffering, CaMKII inhibition, or  $\beta$ -adrenergic stimulation.

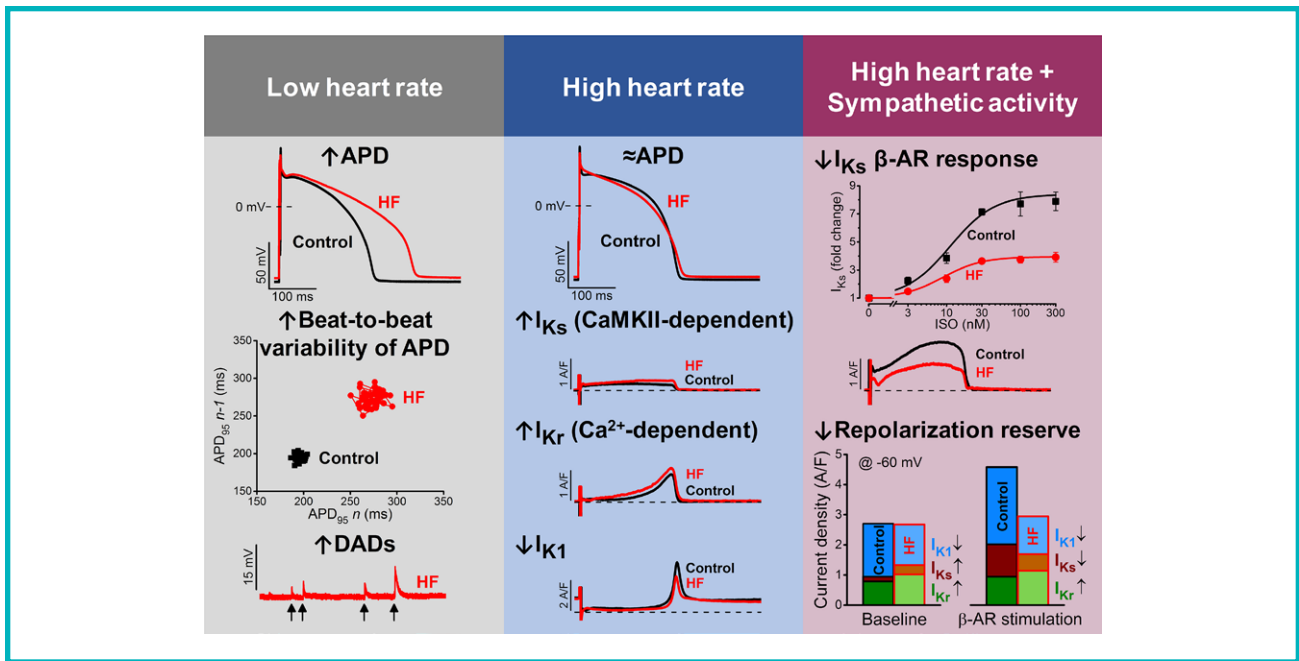
**CONCLUSIONS:** At baseline  $Ca^{2+}$ -dependent upregulation of  $I_{Kr}$  and  $I_{Ks}$  in HF counterbalances the reduced  $I_{K1}$ , maintaining repolarization reserve (especially at higher heart rates) in physiological conditions, unlike conditions of strong cytosolic  $Ca^{2+}$  buffering. However, under  $\beta$ -adrenergic stimulation, reduced  $I_{Ks}$  responsiveness severely limits integrated repolarizing  $K^+$  current and repolarization reserve in HF. This would increase arrhythmia propensity in HF, especially during adrenergic stress.

Bence Hegyi, MD, PhD  
Julie Bossuyt, DVM, PhD  
Kenneth S. Ginsburg, PhD  
Lynette M. Mendoza,  
MBA, RDCS  
Linda Talken  
William T. Ferrier, DVM  
Steven M. Pogwizd, MD  
Leighton T. Izu, PhD  
Ye Chen-Izu, PhD  
Donald M. Bers, PhD

**Correspondence to:** Donald M. Bers, PhD, Department of Pharmacology, University of California, Davis, 451 Health Sciences Dr, Davis, CA 95616. E-mail dmbers@ucdavis.edu

**Key Words:** action potential  
■ calcium/calmodulin-dependent protein kinase II  
■ electrophysiology ■ heart failure  
■ potassium channels

© 2018 American Heart Association, Inc.



### WHAT IS KNOWN?

- Ion channel remodeling occurs in heart failure, resulting in prolongation of the cardiac action potential (and QT interval on the ECG), predominantly at low heart rates.
- Prolonged action potential is associated with increased risk of cardiac arrhythmias.

### WHAT THE STUDY ADDS?

- Calcium/CaMKII (Ca<sup>2+</sup>/calmodulin-dependent protein kinase II)-dependent increases of delayed rectifier K<sup>+</sup> currents (*I<sub>Kr</sub>* and *I<sub>Ks</sub>*) compensate for the decrease of inward rectifier K<sup>+</sup> current (*I<sub>K1</sub>*) in heart failure (at higher heart rates).
- Reduced β-adrenergic responsiveness of *I<sub>Ks</sub>* severely limits repolarization reserve in heart failure during sympathetic stimulation, further increasing arrhythmia risk.

**H**ear failure (HF) is known to induce profound electric remodeling affecting the repolarization process of the cardiac action potential (AP) resulting in increased risk for cardiac arrhythmias. HF patients with prolonged heart rate-corrected QT interval (QT<sub>c</sub>) in their ECG are thought to have higher risk for electric abnormalities and sudden cardiac death,<sup>1-3</sup> although details are debated<sup>4,5</sup> and more than half of HF patients exhibit normal QT<sub>c</sub>.<sup>2-6</sup> Meanwhile, in isolated ventricular myocytes, AP duration (APD) is typically reported to be prolonged both in human HF<sup>7,8</sup> and in animal HF models.<sup>9-12</sup> However, in those studies, APD

prolongation was most pronounced at low pacing rates and when cytosolic Ca<sup>2+</sup> was buffered (ie, nonphysiological conditions). Moreover, no APD prolongation was found above 1 Hz pacing frequency in human,<sup>8</sup> canine,<sup>13</sup> and rabbit<sup>14</sup> failing myocytes, in line with observations that differences in QT intervals between healthy controls and HF patients was abolished at high heart rates.<sup>15</sup>

Earlier studies demonstrated that reduced K<sup>+</sup> currents, enhanced Na<sup>+</sup>/Ca<sup>2+</sup> exchange, and increased late Na<sup>+</sup> currents contribute to APD prolongation in HF.<sup>7-14,16</sup> But these data were obtained in nonphysiological conditions (rectangular voltage clamp pulses versus AP clamp, long cycle lengths, and with cytosolic Ca<sup>2+</sup> transients eliminated by Ca<sup>2+</sup> buffers). In addition to direct Ca<sup>2+</sup> effects on channel gating, CaMKII (Ca<sup>2+</sup>/calmodulin-dependent protein kinase II) activation requires locally high [Ca<sup>2+</sup>]<sub>i</sub> levels. Importantly, CaMKII is also known to be upregulated and more active in HF<sup>17</sup> and has been shown to modulate Na<sup>+</sup> and K<sup>+</sup> channel gating and can also alter channel expression levels<sup>18,19</sup> that shape the cardiac AP and contribute to arrhythmogenesis in HF.<sup>20,21</sup> This regulatory action of CaMKII on ionic currents might have been underestimated in previous HF studies using nonphysiological conditions for recordings.

In this study, we aimed to measure the actual repolarizing K<sup>+</sup> currents that occur under physiological AP-clamp recording conditions to assess the modulatory effect of CaMKII by [Ca<sup>2+</sup>]<sub>i</sub> transients and β-AR (β-adrenergic receptor) activation. We hypothesized that increased [Ca<sup>2+</sup>]<sub>i</sub> and CaMKII activity under physiological conditions play a role in the attenuated AP prolongation at higher pacing rates in HF versus control. Specifically, we

measured APs and 3 major repolarizing K<sup>+</sup> currents during phase 3 of the AP: the rapid and slow components of delayed rectifier K<sup>+</sup> currents ( $I_{Kr}$  and  $I_{Ks}$ , respectively) and the inward rectifier K<sup>+</sup> current ( $I_{K1}$ ) in HF and age-matched control rabbit ventricular myocytes. We used a previously well-characterized chronic nonischemic HF rabbit model (combined volume and pressure overload), which is also arrhythmogenic.<sup>11,17,21–25</sup> We used the AP clamp technique at 2 Hz pacing both with preserved  $[Ca^{2+}]_i$  transients<sup>26,27</sup> and with  $[Ca^{2+}]_i$  buffered below the diastolic level. Modulation of these K<sup>+</sup> currents by Ca<sup>2+</sup>, CaMKII, and  $\beta$ -AR stimulation was also examined to assess the changes of the repolarization reserve in pathophysiological settings characteristic of HF.<sup>11,20</sup>

## METHODS

The data, analytic methods, and study materials will not be made available to other researchers for purposes of reproducing the results or replicating the procedure.

All animal handling and laboratory procedures were in accordance with the approved protocols of the local Institutional Animal Care and Use Committee confirming to the Guide for the Care and Use of Laboratory Animals published by the US National Institute of Health (8th edition, 2011).

### Arrhythmogenic Rabbit Nonischemic HF Model

HF was induced in New Zealand White rabbits (all male, 2.5–3 kg, 3- to 4-month-old) by combined aortic insufficiency and afterward abdominal aortic stenosis as previously described.<sup>22</sup> HF progression was monitored by echocardiography, and myocytes were isolated when left ventricular end-systolic dimension exceeded 1.55 cm (Table). Similar to our previous studies in this rabbit model, the hearts used here were increased in weight by  $\approx 100\%$ , dilated (left ventricular end-diastolic diameter), and exhibited reduced fractional shortening. HF animals also exhibited abdominal ascites fluid and evidence of lung edema (lung weight and lung weight-to-body weight ratio).

For myocyte isolation, rabbits were subjected to general anesthesia (induction with propofol 2 mg/kg followed by 2%–5% isoflurane in 100% oxygen). After thoracotomy, the heart was quickly excised and rinsed in cold nominally Ca<sup>2+</sup>-free Minimum Essential Medium. The right atrium was removed and the aorta opened to visualize the left coronary ostium, which was then cannulated using a 5 F Judkins right catheter (Performa; Merit Medical Systems). Perfusion of the left ventricle and left atrium was established before removal of the right ventricular free wall and application of a purse-string suture to secure the catheter in place. The remainder of the isolation procedure was then essentially as previously described.<sup>28</sup> Cells isolated from healthy age-matched rabbits were used for control experiments.

### Electrophysiology

Isolated cells were transferred to a temperature-controlled plexiglass chamber (Cell Microsystems) and continuously superfused with a bicarbonate containing Tyrode solution

**Table. Morphometric Data of HF and Age-Matched Control Rabbits**

	Age-Matched Control	HF
Age, years	2.40 $\pm$ 0.17	2.46 $\pm$ 0.35*
Body weight, kg	3.99 $\pm$ 0.14	3.98 $\pm$ 0.13*
Heart weight, g	10.46 $\pm$ 0.59	21.86 $\pm$ 2.54†
HW/BW, g/kg	2.63 $\pm$ 0.15	5.52 $\pm$ 0.71‡
Lung weight, g	13.86 $\pm$ 0.25	18.94 $\pm$ 1.16‡
LW/BW, g/kg	3.49 $\pm$ 0.12	4.95 $\pm$ 0.21‡
LVEDD, cm	1.08 $\pm$ 0.07	1.63 $\pm$ 0.11†
LVEDD, cm	1.71 $\pm$ 0.07	2.29 $\pm$ 0.09†
FS, %	36.70 $\pm$ 2.02	28.39 $\pm$ 1.13§

Heart failure was induced in 10 rabbits and progression was assessed periodically by echocardiography. Data of HF rabbits at the time when cardiac myocytes were isolated are compared with 5 age-matched healthy control rabbits. All data represent mean $\pm$ SEM. Unpaired, 2-tailed Student's *t* test. FS indicates fractional shortening calculated as FS=(LVEDD–LVESD)/LVEDD $\times$ 100; HF, heart failure; HW/BW, heart weight-to-body weight ratio; LVEDD, left ventricular end-diastolic diameter; LVESD, left ventricular end-systolic diameter; and LW/BW, lung weight-to-body weight ratio.

\**P*>0.0 (not significant).

†*P*<0.001.

‡*P*<0.01.

§*P*<0.05.

with the following composition (in mmol/L): NaCl 124, NaHCO<sub>3</sub> 25, KCl 4, CaCl<sub>2</sub> 1.2, MgCl<sub>2</sub> 1, HEPES 10, Glucose 10, with pH 7.4. APs and underlying ion currents were recorded in whole-cell configuration of patch-clamp technique. Electrodes were fabricated from borosilicate glass (World Precision Instruments) with tip resistances of 2 to 2.5 M $\Omega$  when filled with internal solution containing (in mmol/L) K-aspartate 110, KCl 25, NaCl 5, Mg-ATP 3, HEPES 10, cAMP 0.002, phosphocreatine-K<sub>2</sub> 10, and EGTA 0.01, with pH 7.2. This composition preserved the physiological  $[Ca^{2+}]_i$  transient and contraction of the myocytes.<sup>29</sup> To study the Ca<sup>2+</sup> dependence of ionic currents in HF,  $[Ca^{2+}]_i$  was buffered to nominally zero by adding 10 mmol/L 1,2-bis(2-aminophenoxy)ethane-*N,N,N',N'*-tetraacetic acid (BAPTA) to the above listed pipette solution. The electrodes were connected to the input of an Axopatch 200B amplifier (Axon Instruments). Outputs from the amplifier were digitized at 50 kHz using Digidata1440A A/D card (Molecular Devices) under software control (pClamp 10). The series resistance was typically 3 to 5 M $\Omega$ , and it was compensated by 85%. Experiments were discarded when the series resistance was high or increased by more than 10% during the experiment. Reported AP voltages are already corrected to the liquid junction potentials. All experiments were conducted at 37 $\pm$ 0.1°C.

APs were recorded in current-clamp experiments where cells were stimulated with suprathreshold depolarizing pulses (2 ms duration) delivered via the patch pipette at various pacing frequencies between 0.2 and 5 Hz. After reaching steady state at each frequency (3 minutes pacing at a given frequency), 50 consecutive APs were recorded to examine the average behavior. APD at 95% of repolarization (APD<sub>95</sub>) was used to assess precisely the influence of sodium-calcium exchanger function—which is known to be altered in HF<sup>22</sup>—on AP profile when measured under physiological conditions.<sup>29</sup> Series of 50 consecutive

APs were analyzed to estimate short-term variability (STV) of APD according to the following formula:  $STV = \frac{\sum(|APD_{i+1} - APD_i|)}{[(n_{beats} - 1) \times \sqrt{2}]}$ , where  $APD_n$  and  $APD_{n+1}$  indicate the durations of the  $i$ th and  $(i+1)$ th APs, and  $n_{beats}$  denotes the number of consecutive beats analyzed.<sup>30,31</sup> Changes in STV are presented as Poincaré plots, where 50 consecutive  $APD_{95}$  values are plotted, each against the duration of the previous AP.

AP-clamp Sequential Dissection experiments were conducted as previously described.<sup>26</sup> All currents were recorded after their specific blocker had reached steady-state effect ( $\approx 2$  minutes perfusion). The following sequence of blockers was used to measure the major K<sup>+</sup> currents: 1  $\mu$ mol/L HMR-1556 for  $I_{Ks}$ , 1  $\mu$ mol/L E-4031 for  $I_{Kr}$ , and 100  $\mu$ mol/L BaCl<sub>2</sub> for  $I_{K1}$ . Experiments were performed both when Ca<sup>2+</sup> cycling was preserved (physiol) and when [Ca<sup>2+</sup>]<sub>i</sub> was buffered below the diastolic level using 10 mmol/L BAPTA in the pipette solution (BAPTA<sub>i</sub>) to compare the Ca<sup>2+</sup> sensitivity of these K<sup>+</sup> currents during AP. To test the effect of CaMKII, cells were pretreated for  $\approx 2$  hours with the specific CaMKII inhibitor, AIP (autocamtide-2-related inhibitory peptide; cell-permeable myristoylated form, 1  $\mu$ mol/L) before starting the experiment, and both the perfusion and pipette solutions were also supplemented with AIP. In experiments examining the effect of  $\beta$ -AR stimulation on K<sup>+</sup> currents, isoproterenol (ISO, 3–300 nmol/L) was applied on AP-clamped cells. When ISO reached a steady-state effect ( $\approx 2$  minutes), then the K<sup>+</sup> current blockers were added to the perfusion solution in a cumulative manner to measure  $I_{Ks}$ ,  $I_{Kr}$ , and  $I_{K1}$ . Experiments were excluded from analysis if significant rundown of L-type Ca<sup>2+</sup> current was observed (in periodic tests) or the membrane current after ISO stimulation did not reach steady state.

Ion currents were normalized to cell capacitance, determined in each cell using short (10 ms) hyperpolarizing pulses from  $-10$  to  $-20$  mV. Cell capacitance was  $191.68 \pm 3.60$  pF in HF ( $n=116$  cells/10 animals) versus  $144.52 \pm 1.45$  pF in age-matched controls (75 cells/5 animals) using 2-sample Student's  $t$  test,  $P < 0.001$ .

Chemicals and reagents were purchased from Sigma-Aldrich, if not specified otherwise. E-4031 and HMR-1556 were from Tocris Bioscience.

## Statistical Analysis

Data are expressed as mean  $\pm$  SEM. The number of cells in each experimental group was reported in the figures and figure captions as  $n$ =number of cells/number of animals. Cells in each group came from at least 3 individual animals. Statistical significance of differences was evaluated using 1-way or 2-way analysis of variance to compare multiple groups, and a Bonferroni posttest was used for pairwise comparisons. Differences were deemed significant if  $P < 0.05$ .

## RESULTS

### Frequency- and Ca<sup>2+</sup>-Dependent Changes of AP in HF

Figure 1 shows representative APs and group analysis in HF and age-matched control (abbreviated as Ctl in

figures) myocytes, and first we consider the physiological case with normal Ca<sup>2+</sup> cycling (physiol; Figure 1A and 1B).  $APD_{95}$  was significantly longer in HF versus control at 1 Hz pacing ( $271.8 \pm 15.2$  versus  $197.8 \pm 6.9$  ms, respectively;  $P < 0.001$ ; Figure 1C). As pacing rate was reduced,  $APD_{95}$  progressively increased in HF, but not in control, making the control–HF difference larger (Figure 1C). The anomalous APD shortening in rabbit ventricle at low pacing rates has been attributed to slowly recovering transient outward K<sup>+</sup> current ( $I_{to,s}$ ) that is normally suppressed at physiological heart rates.<sup>32</sup> Notably, at higher physiological stimulation rates (2–5 Hz),  $APD_{95}$  was not significantly different in HF versus control ( $218.9 \pm 13$  versus  $204.2 \pm 7.7$  ms at 2 Hz in HF and control, respectively).

Buffering [Ca<sup>2+</sup>]<sub>i</sub> to very low levels with 10 mmol/L BAPTA in the pipette (BAPTA<sub>i</sub>) also prevented [Ca<sup>2+</sup>]<sub>i</sub> transients and resulted in longer APD in general compared with the physiological solution (Figure 1C, 1E, and 1F). Moreover, with BAPTA<sub>i</sub>, significant APD prolongation was observed in HF versus control at all pacing frequencies studied (Figure 1C), although the absolute difference became smaller with increasing frequency.

AP plateau height, characterized as mid-plateau potential ( $V_{mid-plateau}$ ) was less positive in HF at all frequencies studied for the BAPTA<sub>i</sub> case and for the physiological case as well (except for 0.2–1 Hz; Figure 1D). The extent of plateau depression at 2 to 5 Hz was greater with buffered [Ca<sup>2+</sup>]<sub>i</sub> than for physiological pipette solution (HF-physiol versus HF-BAPTA<sub>i</sub>; Figure 1D). Consistent with this, early repolarization rate and magnitude (AP phase 1) were both reduced in HF under both pipette conditions (Figure 1A, 1B, 1E, and 1F). Resting membrane potential ( $V_{rest}$ ) was slightly more positive in HF, and AP peak voltage ( $V_{peak}$ ) was significantly lower in HF under both conditions (Figure 1G). In line with this, the AP maximum rate of rise ( $dV/dt_{max}$ ) was also decreased by  $\approx 25\%$  in HF (Figure 1H), which might reflect the altered Na<sup>+</sup> channel availability at more positive  $V_{rest}$ , but contributions of decreased Na<sup>+</sup> channel functional expression or elevated [Na<sup>+</sup>]<sub>i</sub> cannot be ruled out. Importantly here, the maximum rate of repolarization ( $-dV/dt_{max}$ ) during AP phase 3 was also significantly decreased in HF versus control myocytes under physiological conditions and more markedly so with BAPTA<sub>i</sub> (Figure 1H).

HF rabbit myocytes also exhibited increased temporal variability of  $APD_{95}$  compared with myocytes from control hearts (Figure 2A). The STV calculated using 50 consecutive  $APD_{95}$  values was significantly increased at 1 Hz pacing in HF versus control (HF-physiol versus Ctl-physiol,  $4.65 \pm 0.43$  versus  $3.04 \pm 0.23$  ms, respectively;  $P < 0.01$ ), and at 2 Hz as well, where mean  $APD_{95}$  did not differ in HF versus control (Figure 2B). However, these differences became smaller at higher frequencies. We also analyzed the cumulative distribution of beat-to-beat changes in  $APD_{95}$ . More than half of con-

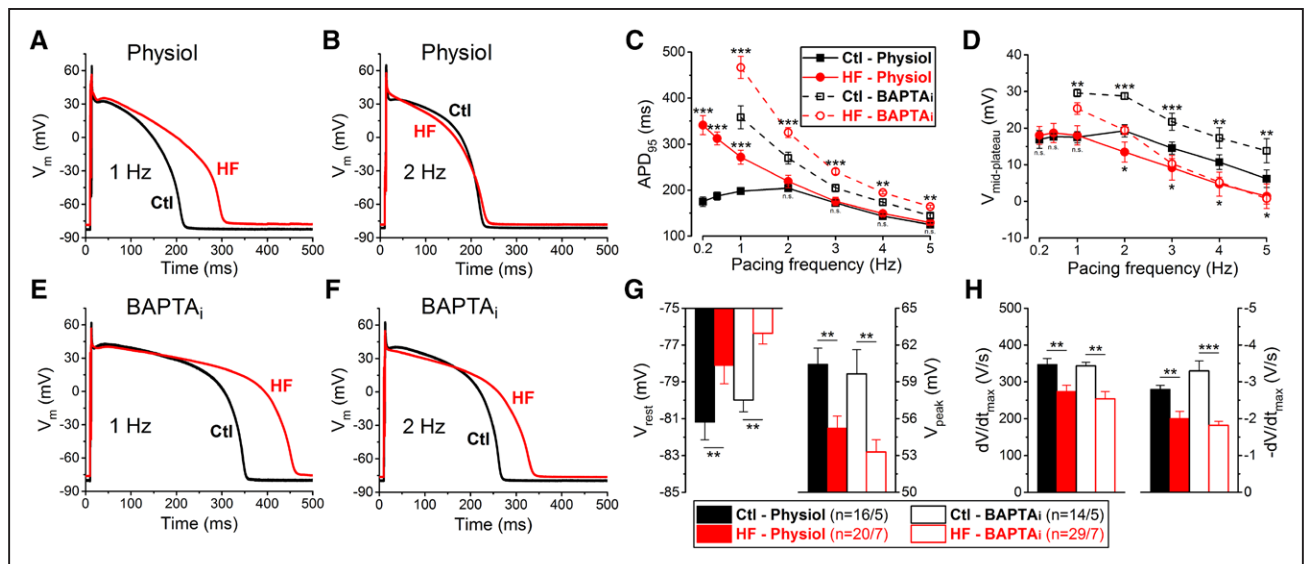


**Figure 1. Frequency- and Ca<sup>2+</sup>-dependent changes of AP parameters in HF.**

**A and B**, Representative action potentials (APs) recorded at 1 and 2 Hz pacing in heart failure (HF) and healthy age-matched control cells with physiological solutions (physiol). **C and D**, Frequency dependence of AP duration (APD) measured at 95% of repolarization (APD<sub>95</sub>) and mid-plateau potential ( $V_{\text{mid-plateau}}$ ). **E and F**, Representative APs when cytosolic Ca<sup>2+</sup> was buffered to nominally zero using 10 mmol/L BAPTA in pipette solution (BAPTA<sub>i</sub>) at 1 and 2 Hz pacing. **G**, Resting membrane potential ( $V_{\text{rest}}$ ) is less negative in HF in line with decreased AP peak ( $V_{\text{peak}}$ ) at 1 Hz. **H**, Both maximal rate of rise ( $dV/dt_{\text{max}}$ ) and maximal rate of phase 3 repolarization ( $-dV/dt_{\text{max}}$ ) are significantly decreased in HF at 1 Hz. Columns and bars represent mean±SEM. *n* refers to cells/animals measured in each group. Analysis of variance (ANOVA) with Bonferroni posttest, Ctl vs HF; \**P*<0.05, \*\**P*<0.01, \*\*\**P*<0.001. Ctl indicates control.

secutive beats have <5 ms difference (both control and HF), but for HF a larger percentage of beats exhibited >5 and 10 ms difference from beat to beat, apparent as long tails in the cumulative distribution curves (Figure 2C and 2D). This difference was less with BAPTA<sub>i</sub>.

Spontaneous sarcoplasmic reticulum (SR) Ca<sup>2+</sup> release (or leak) and consequent afterdepolarizations are known to contribute to increased beat-to-beat variability of APD<sup>30</sup> and are known to occur more frequently in this HF model at a given SR Ca<sup>2+</sup> load (CaMKII-dependently).<sup>17,33,34</sup> However, at baseline in steady-state pacing, neither early nor delayed afterdepolarizations (DAD) were observed in either control or HF. Therefore, to test the SR Ca<sup>2+</sup> store stability, we paced the cells at 2 Hz for 5 minutes, then paused to record  $V_m$  without stimulation. DADs developed in 10/12 HF cells, and among them, 5 cells also exhibited spontaneous APs likely to be triggered by SR Ca release (Figure 2E shows an example). Average DAD frequency was 1.14±0.31/min, with average amplitude of 3.15±0.19 mV. Only 15% of DADs were larger than 5 mV in amplitude (not including those that triggered APs). However, neither the age-matched controls cells (0/12 cells) nor HF cells pretreated with CaMKII inhibitory peptide AIP (1 μmol/L; 0/10 cells) showed such arrhythmogenic activities (Figure 2E). Thus, higher SR Ca<sup>2+</sup> instability may contribute to the higher beat-to-beat APD variability in HF (Figure 2C and 2D) that was suppressed by BAPTA<sub>i</sub>.

### Changes in Magnitude and Dynamics of $I_{Kr}$ , $I_{Ks}$ , and $I_{K1}$ Under AP in HF

The APD data suggest complex remodeling in HF and the involvement of Ca<sup>2+</sup>-dependent processes in the altered repolarization phase at higher physiological rabbit pacing rates. Thus, we studied the major repolarizing K<sup>+</sup> currents ( $I_{Kr}$ ,  $I_{Ks}$ , and  $I_{K1}$ ) during phase 3 of the AP at 2 Hz. All 3 ionic currents were recorded from the same myocyte using the AP-clamp Sequential Dissection technique<sup>26</sup> with preserved [Ca<sup>2+</sup>]<sub>i</sub> cycling condition (Physiol) and also with [Ca<sup>2+</sup>]<sub>i</sub> buffered with 10 mmol/L BAPTA in the pipette (BAPTA<sub>i</sub>). Involvement of CaMKII pathway was also investigated in the Ca<sup>2+</sup>-dependent alteration of repolarization. A previously recorded typical rabbit ventricular AP was used as voltage command in all AP-clamp experiments (canonical AP-clamp) at 2 Hz. This typical AP has an APD<sub>95</sub> of 205.5 ms, which is not significantly different from the APD<sub>95</sub> of either control or HF cells at 2 Hz (one sample *t* test). Because significant cellular hypertrophy was found in HF (~33% increase in cell capacitance, see Methods for details), all reported currents are normalized to the corresponding cell capacitance.

The rapid component of delayed rectifier potassium current ( $I_{Kr}$ ) was measured as E-4031-sensitive current under AP clamp (Figure 3A through 3C). Peak  $I_{Kr}$  density was 18% higher in HF myocytes compared with age-matched controls when measured in our physiological

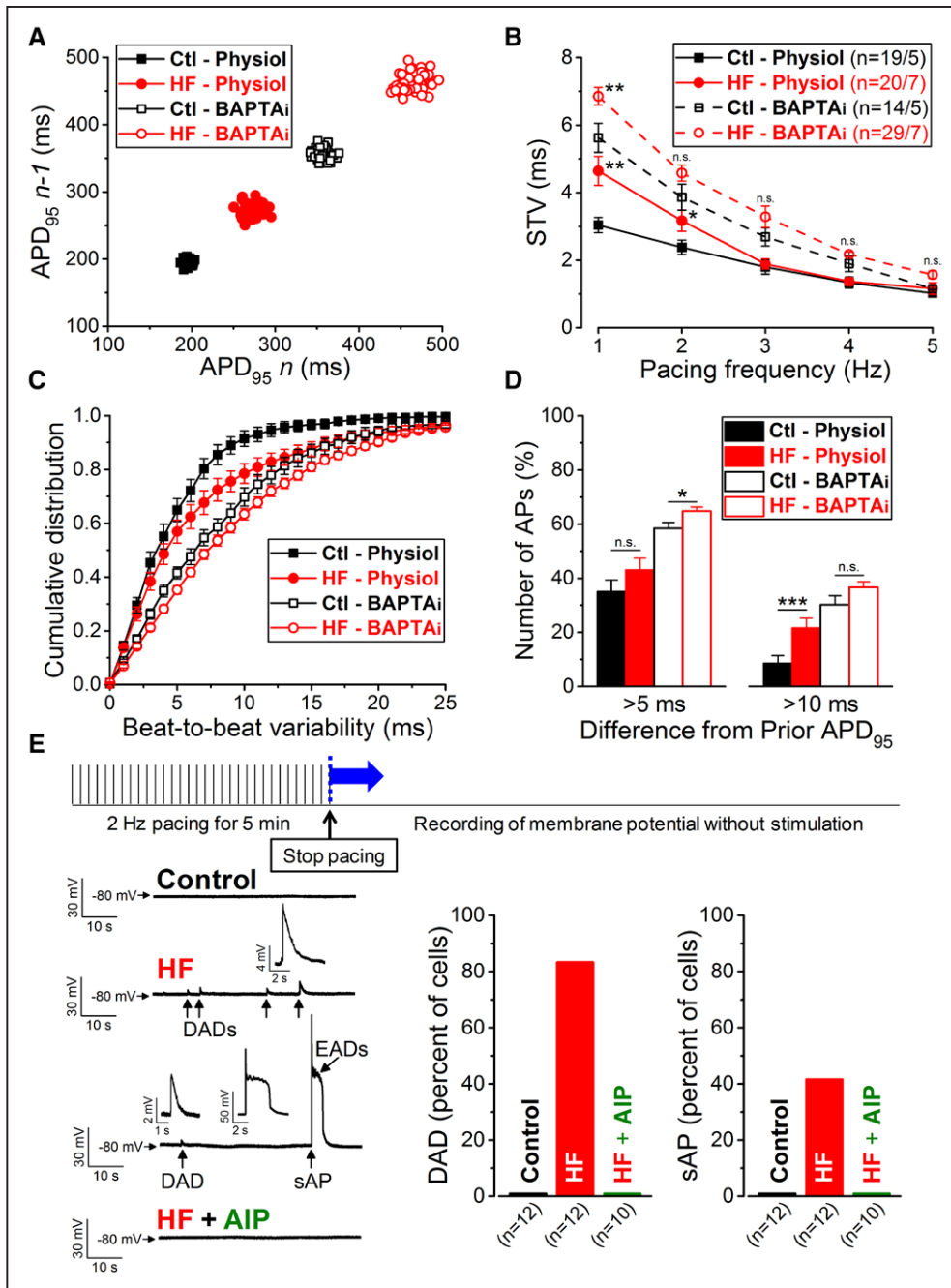


**Figure 2. Increased temporal variability of action potential duration (APD) and arrhythmogenesis in heart failure (HF).**

**A**, Representative Poincaré plots of 50 consecutive APD<sub>95</sub> values at 1 Hz steady-state pacing in 4 individual myocytes from HF and age-matched control animals recorded with either preserved or buffered [Ca<sup>2+</sup>]<sub>i</sub>. **B**, Frequency-dependent short-term variability of APD<sub>95</sub> (STV). **C**, Cumulative distribution curves of individual beat-to-beat variability values at 1 Hz pacing. **D**, Percentage of total action potentials (APs) measured at 1 Hz pacing having beat-to-beat APD<sub>95</sub> variability of >5 and >10 ms in consecutive beats. Columns and bars represent mean±SEM. *n* refers to cells/animals measured in each group. Analysis of variance (ANOVA) with Bonferroni posttest, \**P*<0.05, \*\**P*<0.01, \*\*\**P*<0.001. **E**, Arrhythmogenic diastolic activities were tested using the pacing protocol shown above. **Left**, Representative records in control, HF, and AIP (autocamtide-2-related inhibitory peptide; CaMKII [Ca<sup>2+</sup>/calmodulin-dependent protein kinase II] inhibitor, 1 μmol/L)-treated HF cells are shown below. HF cells frequently showed delayed afterdepolarizations (DADs, enlarged in insets) and spontaneous AP (sAP, enlarged in inset). Early afterdepolarizations (EADs, enlarged in inset) were also superimposed on the sAP repolarization. **Right**, Percentage of cells having DAD and sAP. Ten of 12 cells and 5/12 cells showed DADs and sAP in HF, respectively, whereas no DAD, sAP, or EAD was observed in control and after AIP treatment in HF.

condition ( $1.13 \pm 0.02$  versus  $0.96 \pm 0.02$  A/F in HF and control, respectively;  $P < 0.001$ ; Figure 3A and 3D). In contrast, with BAPTA<sub>i</sub>, peak  $I_{Kr}$  density was 7% smaller in HF versus control ( $0.86 \pm 0.02$  versus  $0.92 \pm 0.02$  A/F, respectively;  $P < 0.05$ ; Figure 3B and 3D). AIP pretreatment to inhibit CaMKII affected neither peak  $I_{Kr}$  density nor integrated charge carried by  $I_{Kr}$  in either control or HF (Figure 3C, 3D, and 3F), suggesting that CaMKII is not involved in acute  $I_{Kr}$  modulation. On the other hand,  $I_{Kr}$  is elevated earlier during the AP in HF versus control (Figure 3E), regardless of  $[Ca^{2+}]_i$  (Figure 3A versus Figure 3B and 3E), indicating altered  $I_{Kr}$  gating in HF. The slight increase in peak and integrated  $I_{Kr}$  under physiological conditions here could easily be missed if  $I_{Kr}$  is measured under nonphysiological conditions (eg, BAPTA<sub>i</sub>).

The slow component of delayed rectifier K<sup>+</sup> current ( $I_{Ks}$ ) was measured as HMR-1556-sensitive current

under AP clamp (Figure 4A through 4C).  $I_{Ks}$  is a tiny current in the absence of  $\beta$ -AR stimulation in healthy ventricular myocytes (Figure 4A), consistent with minimal effects of  $I_{Ks}$  block on baseline APD in rabbit ventricle.<sup>35</sup> Surprisingly, we found a 42% increase in basal  $I_{Ks}$  magnitude in HF versus control in our physiological condition ( $0.34 \pm 0.03$  versus  $0.24 \pm 0.02$  A/F, respectively;  $P < 0.01$ ; Figure 4A and 4D through 4F). Furthermore, the increase in  $I_{Ks}$  was not observed with BAPTA<sub>i</sub> (Figure 4B) or when HF cells were pretreated with AIP (Figure 4C through 4F). We infer that Ca<sup>2+</sup>-dependent CaMKII activity may acutely increase  $I_{Ks}$  in HF.

The inward rectifier K<sup>+</sup> current ( $I_{K1}$ ) was measured as Ba<sup>2+</sup>-sensitive current (Figure 5A through 5C). Peak  $I_{K1}$  density during repolarization was 25% smaller in HF versus control ( $2.28 \pm 0.11$  versus  $3.04 \pm 0.12$  A/F, respectively;  $P < 0.001$ ; Figure 5A and 5D). Mid-plateau

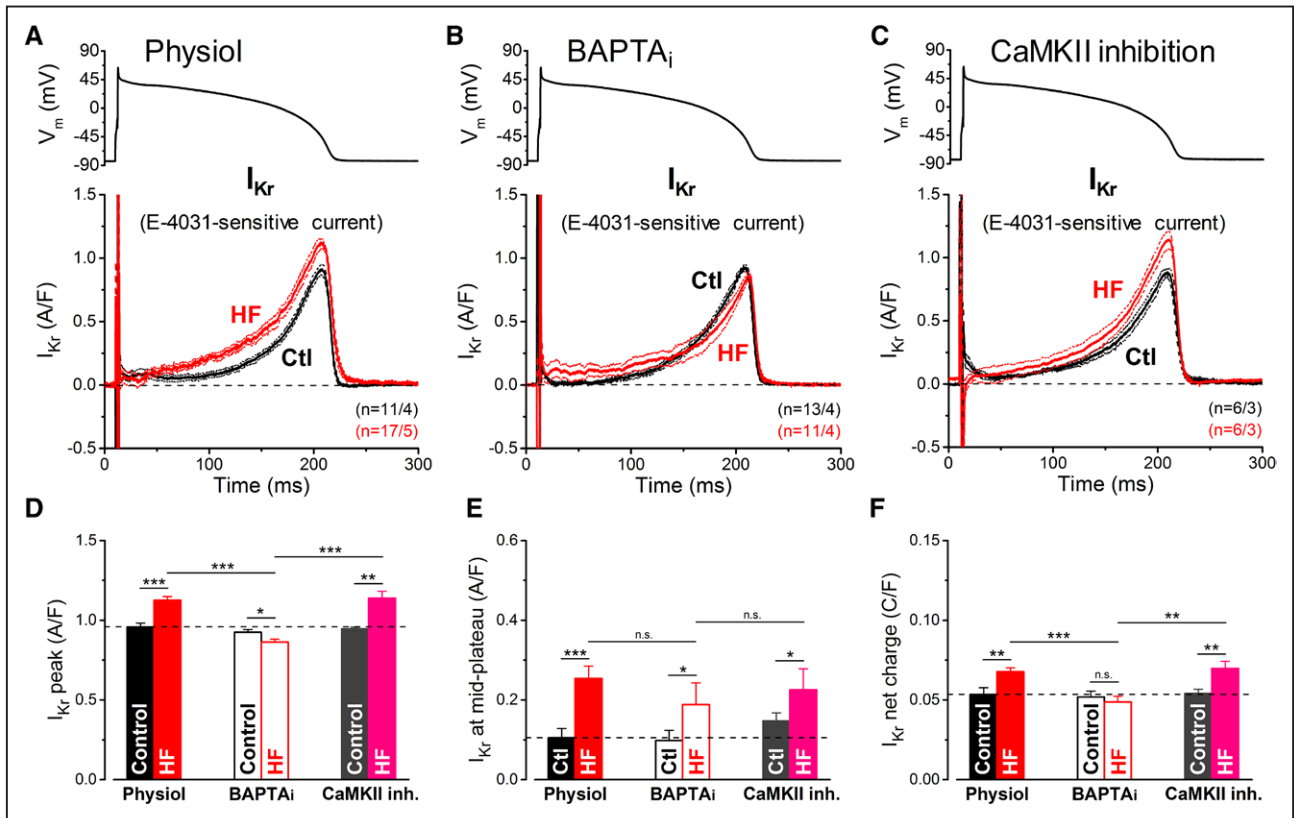


**Figure 3. Ca<sup>2+</sup>-dependent upregulation of  $I_{Kr}$  in heart failure (HF) under action potential (AP) clamp.**

The rapid component of delayed rectifier K<sup>+</sup> current ( $I_{Kr}$ ) was measured as E-4031 (1  $\mu$ mol/L)-sensitive current in HF and age-matched control cells. AP clamp using a prerecorded typical AP (shown above) was applied at 2 Hz. **A**,  $I_{Kr}$  traces (mean  $\pm$  SEM) recorded under preserved  $[Ca^{2+}]_i$  cycling (physiol).  $I_{Kr}$  is not only increased in HF cells having  $[Ca^{2+}]_i$  transients, but it activates earlier during the AP. **B**,  $I_{Kr}$  traces (mean  $\pm$  SEM) recorded under buffered  $[Ca^{2+}]_i$  using 10 mmol/L BAPTA in the pipette (BAPTA<sub>i</sub>). Buffering  $[Ca^{2+}]_i$  significantly reduced  $I_{Kr}$  density in HF below the control level, but it had no effect in control. **C**,  $I_{Kr}$  traces (mean  $\pm$  SEM) recorded in cells pretreated with the specific CaMKII (Ca<sup>2+</sup>/calmodulin-dependent protein kinase II) inhibitor peptide AIP (autocamtide-2-related inhibitory peptide; 1  $\mu$ mol/L). AIP had no effect on  $I_{Kr}$  both in control and in HF. **D**, Peak  $I_{Kr}$  density is significantly upregulated in HF under AP by a Ca<sup>2+</sup>-dependent, but CaMKII-independent pathway. **E**,  $I_{Kr}$  density measured at the mid-plateau increased in HF, indicating earlier  $I_{Kr}$  accumulation during AP, which occurred independent of  $[Ca^{2+}]_i$  level and CaMKII activity. **F**, Net charges carried by  $I_{Kr}$  in HF and age-matched control. Columns and bars represent mean  $\pm$  SEM. *n* refers to cells/animals measured in each group. Analysis of variance (ANOVA) with Bonferroni posttest, \* $P < 0.05$ , \*\* $P < 0.01$ , \*\*\* $P < 0.001$ .

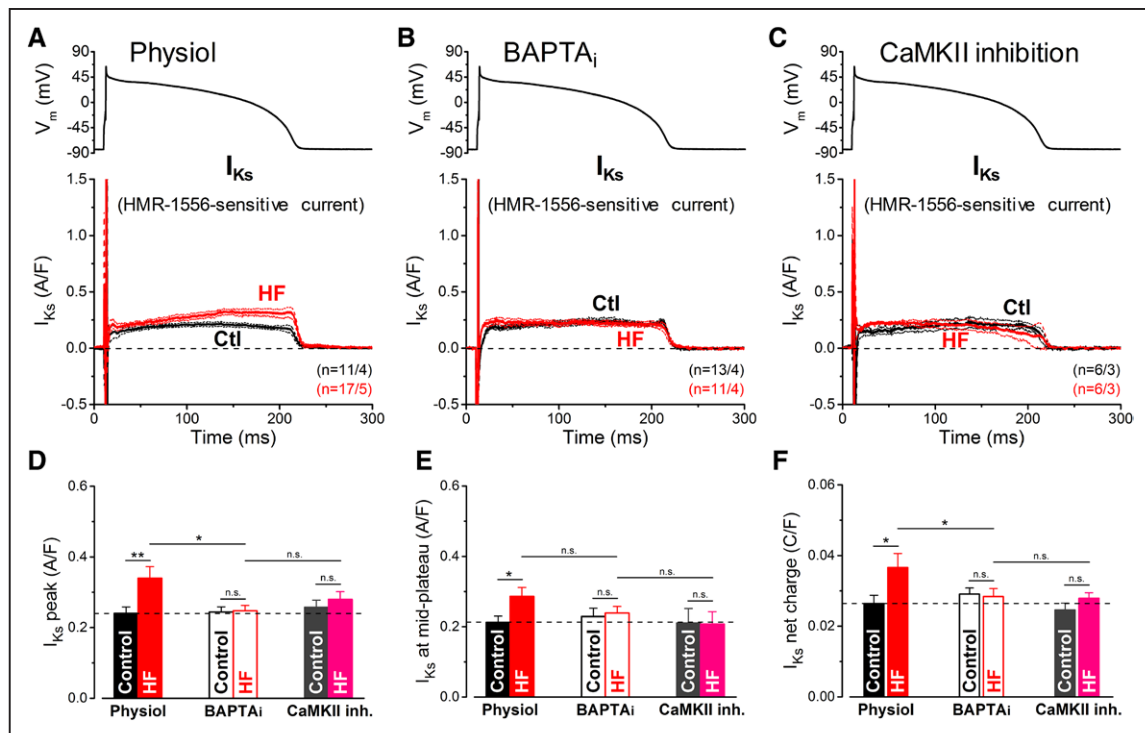


**Figure 4.** Ca<sup>2+</sup>/CaMKII (Ca<sup>2+</sup>/calmodulin-dependent protein kinase II)-dependent upregulation of  $I_{Ks}$  in heart failure (HF) under action potential (AP) clamp.

The slow component of delayed rectifier K<sup>+</sup> current ( $I_{Ks}$ ) was measured as HMR-1556 (1  $\mu$ mol/L)-sensitive current in HF and age-matched control cells. AP clamp using a prerecorded typical AP (shown above) was applied at 2 Hz. **A**,  $I_{Ks}$  traces (mean $\pm$ SEM) recorded under preserved [Ca<sup>2+</sup>]<sub>i</sub> cycling (physiol). Basal  $I_{Ks}$  is a tiny current under AP, yet it is significantly upregulated in HF cells having [Ca<sup>2+</sup>]<sub>i</sub> transients. **B**,  $I_{Ks}$  traces (mean $\pm$ SEM) recorded under buffered [Ca<sup>2+</sup>]<sub>i</sub> using 10 mmol/L BAPTA in the pipette (BAPTA<sub>i</sub>). Buffering [Ca<sup>2+</sup>]<sub>i</sub> reduced  $I_{Ks}$  in HF back to its control level. **C**,  $I_{Ks}$  traces (mean $\pm$ SEM) recorded in cells pretreated with the specific CaMKII inhibitor peptide AIP (autocamtide-2-related inhibitory peptide; 1  $\mu$ mol/L). AIP abolished the  $I_{Ks}$  upregulation in HF. **D**, Peak  $I_{Ks}$  density is significantly upregulated in HF under AP by a Ca<sup>2+</sup>/CaMKII-dependent pathway. **E**,  $I_{Ks}$  density measured at the mid-plateau of the AP. **F**, Net charges carried by  $I_{Ks}$  in HF and age-matched control. Columns and bars represent mean $\pm$ SEM. *n* refers to cells/animals measured in each group. Analysis of variance (ANOVA) with Bonferroni posttest, \**P*<0.05, \*\**P*<0.01.

and integrated  $I_{K1}$  over the APD was also smaller in HF versus control (Figure 5E through 5F). Neither buffering [Ca<sup>2+</sup>]<sub>i</sub> (BAPTA<sub>i</sub>) nor CaMKII inhibition (AIP) altered this conclusion (Figure 5B and 5C). We conclude that  $I_{K1}$  downregulation in this HF model is not mainly caused by acute effects of [Ca<sup>2+</sup>]<sub>i</sub> or CaMKII on  $I_{K1}$ , but might reflect lower functional expression level of the channel proteins. Because CaMKII is upregulated in HF<sup>17</sup> and can cause reduced functional expression of K<sub>v</sub>2.1 and  $I_{K1}$ ,<sup>19</sup> this does not preclude an indirect chronic effect of CaMKII on  $I_{K1}$  functional expression in HF.

### Altered $\beta$ -Adrenergic Response of K<sup>+</sup> Currents in HF

Increased sympathetic activation and altered  $\beta$ -AR responses are frequently reported in HF. Therefore, we also tested effects of  $\beta$ -AR stimulation on  $I_{Kr}$ ,  $I_{Ks}$ , and  $I_{K1}$  in HF and control myocytes using AP clamp. Because both PKA (protein kinase A) and CaMKII are known to mediate downstream effects of  $\beta$ -AR stimulation

and the activity of these kinases are also known to be altered in HF, we again measured ionic currents with physiological preserved [Ca<sup>2+</sup>]<sub>i</sub> cycling and with heavily buffered [Ca<sup>2+</sup>]<sub>i</sub>.

$I_{Ks}$  increased robustly on treatment with the non-specific  $\beta$ -AR agonist ISO (10 nmol/L; Figure 6A and 6D). Buffering [Ca<sup>2+</sup>]<sub>i</sub> limited  $I_{Ks}$  response, indicating the involvement of Ca<sup>2+</sup> and CaMKII (as well as PKA) in mediating ISO effect on  $I_{Ks}$ . However, the ISO-induced increase in  $I_{Ks}$  peak density was much reduced in HF both with [Ca<sup>2+</sup>]<sub>i</sub> cycling (7.25-fold in control versus 2.91-fold increase in HF) and with BAPTA<sub>i</sub> (3.85-fold in control versus 2.88-fold in HF; Figure 6D). The ISO-induced increase in  $I_{Ks}$  in the presence of Ca<sup>2+</sup> was not simply a scaled-up version of the BAPTA<sub>i</sub> traces, but a more prominent increase during the plateau, resulting in an even greater increment in integrated charge carried by  $I_{Ks}$  (Figure 6A and 6D). Even after ISO, the integrated K<sup>+</sup> efflux during the AP in HF was less than half of that in control (Figure 6D), which could seriously limit repolarization reserve.

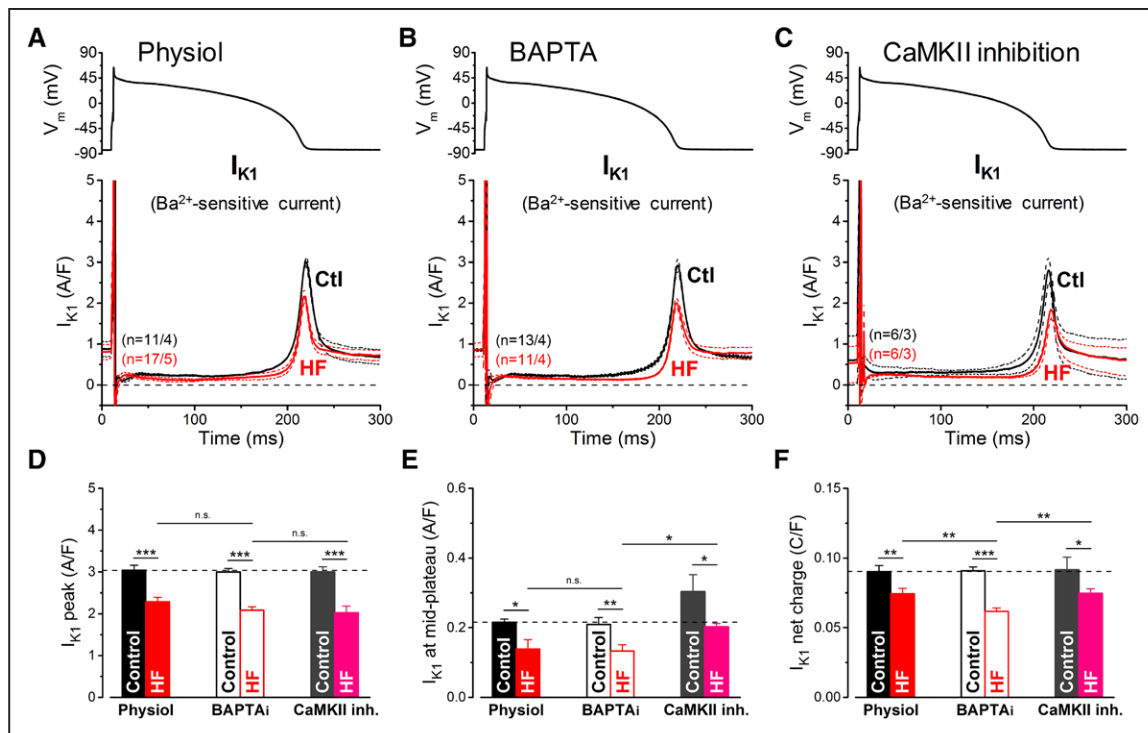


**Figure 5. Reduction of  $I_{K1}$  in heart failure (HF) under action potential (AP) clamp.**

The inward rectifier K<sup>+</sup> current ( $I_{K1}$ ) was measured as Ba<sup>2+</sup> (100 μmol/L)-sensitive current in HF and age-matched control cells. AP clamp using a prerecorded typical AP (shown above) was applied at 2 Hz. **A–C**,  $I_{K1}$  traces (mean±SEM) recorded under preserved [Ca<sup>2+</sup>]<sub>i</sub> cycling (physiol), [Ca<sup>2+</sup>]<sub>i</sub> buffering (BAPTA), and CaMKII (Ca<sup>2+</sup>/calmodulin-dependent protein kinase II) inhibition using AIP (autocamide-2-related inhibitory peptide).  $I_{K1}$  was significantly reduced in HF in all these conditions. **D–F**, Statistics for peak  $I_{K1}$  density shows that the reduction is not influenced by [Ca<sup>2+</sup>]<sub>i</sub> buffering or acute CaMKII inhibition. **E**,  $I_{K1}$  density measured at the mid-plateau of the AP was also reduced. **F**, Net charges carried by  $I_{K1}$  was further reduced in HF when measured with [Ca<sup>2+</sup>]<sub>i</sub> buffering. Columns and bars represent mean±SEM. *n* refers to cells/animals measured in each group. Analysis of variance (ANOVA) with Bonferroni posttest, \**P*<0.05, \*\**P*<0.01, \*\*\**P*<0.001.

$I_{Kr}$  was affected minimally on ISO stimulation (Figure 6B and 6E), which achieved statistical significance only in control cells and physiological solutions (8.1% increase in  $I_{Kr}$  peak density and 23.1% increase in total charge carried during the AP, *P*<0.05 in both cases). As in Figure 3,  $I_{Kr}$  was higher at baseline in HF versus control, but failed to increase significantly on ISO exposure (Figure 6E).

$I_{K1}$  peak density was not affected by β-adrenergic stimulation (Figure 6C and 6F). However, the  $I_{K1}$  net charge increased significantly (by 23%) after ISO application in control, but not in HF cells, when measured with cycling [Ca<sup>2+</sup>]<sub>i</sub> under AP clamp (Figure 6F), possibly reflecting some Ca<sup>2+</sup>-dependent rectification of  $I_{K1}$  as previously described.<sup>27,36</sup>

Because the ISO effect on  $I_{Ks}$  was blunted in HF versus control, we tested whether the β-AR effects were because of decreased ISO sensitivity or limited maximal response. We varied ISO between 3 and 300 nmol/L in AP-clamped HF and control cells (Figure 7). Because steady-state contracting AP-clamped myocytes were unstable at the higher ISO concentrations without [Ca<sup>2+</sup>]<sub>i</sub> buffering, these experiments were performed with 10 mmol/L

BAPTA in the pipette. ISO dose-dependently increased  $I_{Ks}$  both in control and HF cells with nearly identical half maximal effective concentration (EC<sub>50</sub>) values (8.39±0.85 and 8.90±1.61 nmol/L, respectively, NS) and Hill coefficients (Figure 7A). However, the maximum response was only half as much in HF versus control (4.0-fold versus 8.4-fold increase in peak  $I_{Ks}$  density, respectively), indicating unchanged ISO sensitivity, but significant hypo-responsiveness of  $I_{Ks}$  to ISO.  $I_{Kr}$  increased only after ISO application, and no difference was seen between control and HF regarding EC<sub>50</sub> values and maximal responses (Figure 7B). Finally, peak  $I_{K1}$  density during the AP did not show any change, even at high concentration of ISO, but  $I_{K1}$  was again significantly reduced in HF (Figure 7C).

### Relative Contributions of Each K<sup>+</sup> Current to AP Phase 3 Repolarization

AP repolarization is governed by the dynamic time- and voltage-dependent activation of K<sup>+</sup> currents. Each K<sup>+</sup> current has its unique fingerprint (current shape under the changing voltages of AP) and different magnitude during the cardiac AP. The relative contributions of the

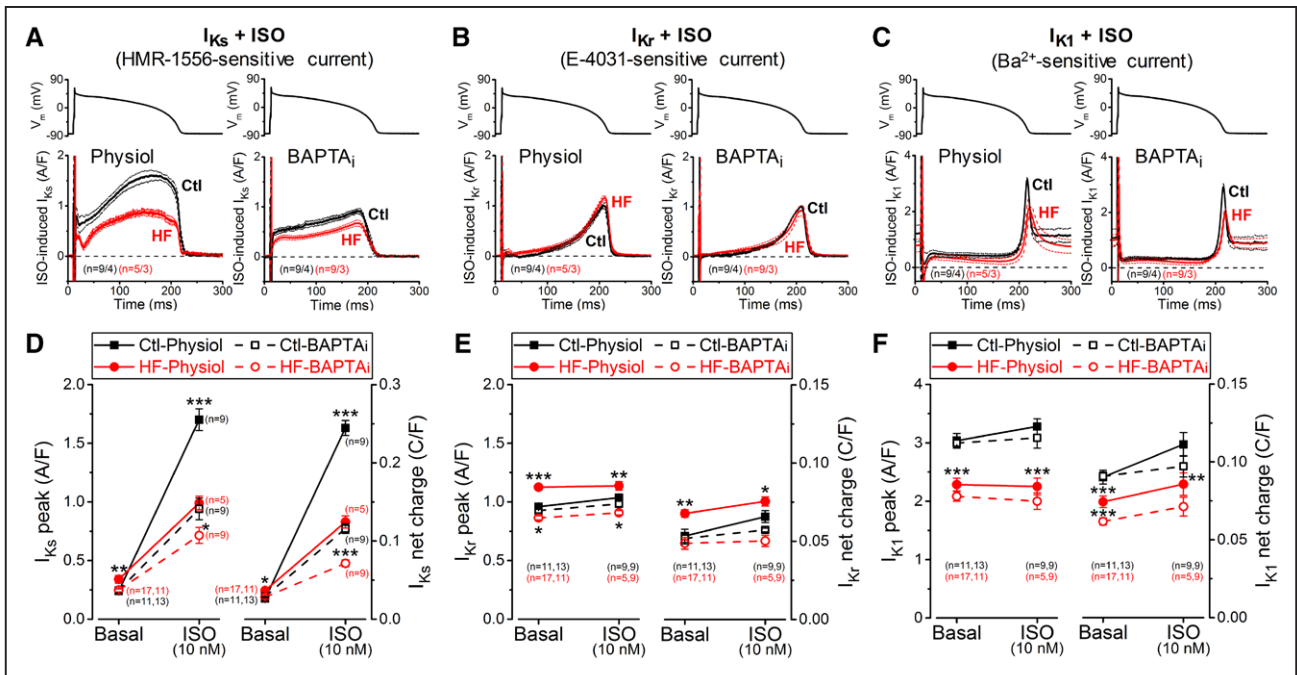


**Figure 6. Altered response of K<sup>+</sup> currents to  $\beta$ -AR ( $\beta$ -adrenergic receptor) stimulation in heart failure (HF).**

$I_{Ks}$ ,  $I_{Kr}$ , and  $I_{K1}$  currents were recorded after 2 minutes pretreatment with  $\beta$ -adrenergic receptor agonist isoproterenol (ISO, 10 nmol/L). **A**,  $I_{Ks}$  traces (mean $\pm$ SEM) under canonical AP clamp at 2 Hz measured with preserved [Ca<sup>2+</sup>]<sub>i</sub> cycling (physiol) and [Ca<sup>2+</sup>]<sub>i</sub> buffering using 10 mmol/L BAPTA in the pipette (BAPTA<sub>i</sub>). **B**,  $I_{Kr}$  traces (mean $\pm$ SEM) under AP clamp after ISO pretreatment in HF and age-matched control cells. **C**,  $I_{K1}$  traces (mean $\pm$ SEM) under AP clamp after ISO pretreatment in physiological solutions and in BAPTA<sub>i</sub>. **D**, Robust upregulation of  $I_{Ks}$  peak and net charge induced by ISO, which is reduced in BAPTA<sub>i</sub>, indicating a Ca<sup>2+</sup>-dependent pathway in mediating the response of  $\beta$ -AR stimulation on  $I_{Ks}$  besides the classical PKA (protein kinase A)-dependent phosphorylation. HF cells showed significantly reduced  $I_{Ks}$  accumulation on ISO application both with and without [Ca<sup>2+</sup>]<sub>i</sub> buffering. **E**,  $I_{Kr}$  is slightly modulated by ISO both in control and HF. **F**,  $I_{K1}$  peak density is not influenced by ISO, but  $I_{K1}$  net charge is slightly increased in HF because of altered rectification. Symbols and bars represent mean $\pm$ SEM. *n* refers to cells measured in each group, and the cells in each group came from 3 to 5 individual animals. Analysis of variance (ANOVA) with Bonferroni posttest, \**P*<0.05, \*\**P*<0.01, \*\*\**P*<0.001.

major K<sup>+</sup> currents ( $I_{Kr}$ ,  $I_{Ks}$  and  $I_{K1}$ ) involved in the phase 3 repolarization of AP in control and in HF are shown in Figure 8 analyzed at different points of repolarization (+20, -20, and -60 mV) and as integrated K<sup>+</sup> flux during the AP (Figure 8, insets).

First, we consider physiological solutions with Ca<sup>2+</sup> cycling at baseline (Figure 8A and 8B) where total repolarizing K<sup>+</sup> current is unaltered in HF versus control at either -20 mV, -60 mV, or the integral. However, the reduced  $I_{K1}$  in HF is largely compensated by increases in both  $I_{Kr}$  and  $I_{Ks}$ , and this balance may allow the relatively maintained APD<sub>95</sub> observed in HF myocytes at 2 to 5 Hz stimulation (Figure 1B and 1C). In control myocytes, ISO greatly increases  $I_{Ks}$  and reverses the  $I_{Kr}$  versus  $I_{Ks}$  dominant pattern of AP repolarization. However, in HF myocytes hyporesponsive of  $I_{Ks}$  to  $\beta$ -AR stimulation,  $I_{Ks}$  remains less than  $I_{Kr}$ , such that the combined  $I_{Ks}+I_{Kr}$  do not compensate for the reduced  $I_{K1}$ , and integrated K<sup>+</sup> current is substantially reduced in HF (Figure 8C).

CaMKII inhibition with AIP affected only  $I_{Ks}$  but because basal  $I_{Ks}$  is a tiny current under physiological AP, it does not significantly alter the magnitude of the net

K<sup>+</sup> current (Figure 8D). Buffering cytosolic Ca<sup>2+</sup> below diastolic level abolishes the upregulation of both  $I_{Kr}$  and  $I_{Ks}$  in HF, resulting in a pronounced decrease in net K<sup>+</sup> current (Figure 8E). ISO in the presence of BAPTA<sub>i</sub> exacerbated the difference between HF and control because under those conditions  $I_{K1}$ ,  $I_{Ks}$ , and  $I_{Kr}$  are all reduced in HF compared with control (Figure 8F).

## DISCUSSION

### APD Changes in HF

There is consensus that HF is associated with lengthening of the ventricular APD (and QT<sub>c</sub>). This is supported by evidence from numerous experimental studies involving several species and multiple methods to induce HF.<sup>7-14</sup> However, HF-associated APD differences in previous studies often used lower pacing rates. In humans, HF was associated with a 50 ms difference in baseline QT<sub>c</sub>, but as heart rate increased during exercise, the QT<sub>c</sub> values converged and were not different between control and HF.<sup>15</sup> In agreement with these observations, we

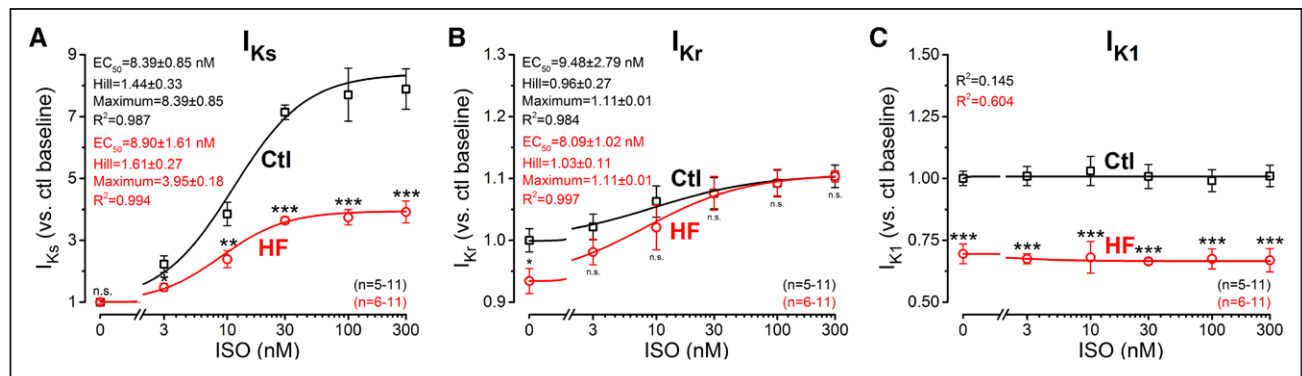


**Figure 7.  $\beta$ -AR ( $\beta$ -adrenergic receptor) responsiveness of K<sup>+</sup> currents in heart failure (HF).**

Dose–response effect of isoproterenol (ISO) on  $I_{Ks}$ ,  $I_{Kr}$ , and  $I_{K1}$  peak densities under AP clamp at 2 Hz. Pipette solution contained 10 mmol/L BAPTA. **A**,  $I_{Ks}$  measured as HMR-sensitive current showed a robust accumulation after ISO application.  $I_{Ks}$  sensitivity ( $EC_{50}$ ) to ISO was unchanged in HF, whereas the response was significantly reduced in HF. **B**,  $I_{Kr}$  was minimally affected by ISO treatment; however, neither the ISO sensitivity nor the magnitude of the response were altered in HF. **C**,  $I_{K1}$  peak density did not change after ISO application under buffered  $[Ca^{2+}]_i$  conditions, and  $I_{K1}$  was uniformly decreased in HF.  $EC_{50}$  values, Hill coefficients, and maximum responses were determined by fitting data to the Hill equation, indicated by solid lines. Symbols and bars represent mean  $\pm$  SEM.  $n$  refers to the number of cells measured in each group, and the cells in each group came from 3 to 5 individual animals. Analysis of variance (ANOVA) with Bonferroni posttest, \* $P < 0.05$ , \*\* $P < 0.01$ , \*\*\* $P < 0.001$ .

found longer APD in HF versus control in rabbits at 0.2 to 1 Hz pacing, but not at higher physiological pacing rates for rabbits (Figure 1). However, when the  $[Ca^{2+}]_i$  was buffered, APD was prolonged in HF at all stimulation rates, suggesting a role for  $Ca^{2+}$ -dependent processes in shaping the AP morphology in HF.

Patients with  $QT_c$  prolongation have increased risk for sudden cardiac death almost independent of the cause of disease.<sup>37</sup> Substantial  $QT_c$  prolongation, especially in end-stage HF and in ischemic origin, indicates higher risk for cardiac arrhythmias also in HF.<sup>4</sup> However, data also suggest that short-term  $QT_c$  variability may be a better predictor of sudden cardiac death than  $QT_c$  interval per se.<sup>5,38</sup> In our arrhythmogenic HF model, STV of  $APD_{95}$  was also significantly increased (Figure 2). It was reported that STV depends critically on the baseline  $APD_{95}$ .<sup>31</sup> In our case, STV was increased in HF versus control at 2 Hz pacing, despite no difference in baseline  $APD_{95}$ . Interestingly, in our HF data, a higher fraction of APs showed large difference in  $APD_{95}$  in subsequent beats (Figure 2C and 2D), despite unaltered mean  $APD_{95}$ . Because strong  $[Ca^{2+}]_i$  buffering suppressed this effect, it seems likely because of  $Ca^{2+}$ -related events (eg, SR  $Ca^{2+}$  releases) rather than remodeling in ionic currents and their different contribution to STV.<sup>31</sup> Accordingly, spontaneous SR  $Ca^{2+}$  leak,  $Ca^{2+}$  sparks, and waves can contribute to increased beat-to-beat variability.<sup>30</sup> Even without overt early afterdepolarization or DAD induction during steady-state pacing, local  $Ca^{2+}$  events could readily cause APD variations. Indeed, we saw such events after trains of stimuli in HF that were prevented by CaMKII inhibition and were not seen in control cells. This is consistent with higher SR  $Ca^{2+}$  leak and  $Ca^{2+}$  waves measured in this arrhythmogenic

rabbit HF model (at matched SR  $Ca^{2+}$  load), which was also sensitive to CaMKII inhibition.<sup>17,24,33,34,39</sup> This higher SR  $Ca^{2+}$  leak associated with HF may contribute to increased beat-to-beat variability of APD; however, further studies are needed to define the precise relationship between these 2 important parameters of HF.

### Changes in Repolarizing K<sup>+</sup> Currents in HF that Shape the AP

In this study, we systematically characterize the major K<sup>+</sup> currents ( $I_{Kr}$ ,  $I_{Ks}$ , and  $I_{K1}$ ) underlying phase 3 AP repolarization in control and HF myocytes, including  $Ca^{2+}$ - and  $\beta$ -AR-dependent properties. Decreased transient outward K<sup>+</sup> current ( $I_{to}$ ) in HF has been reported in several models, including ours.<sup>7,11,40</sup> Consistent with that, we saw reduced phase 1 AP repolarization in HF (Figure 1). However, our focus here is on the K<sup>+</sup> currents that dominate phase 3 repolarization.

To understand how  $I_{Kr}$ ,  $I_{Ks}$ , and  $I_{K1}$  are altered in shaping the APD in HF, we used our sequential dissection method that allows all 3 K<sup>+</sup> currents to be measured in the same myocyte under relatively physiological AP conditions. Often these individual currents are measured independently, with square voltage clamp pulses and under relatively nonphysiological conditions, including prevention of  $[Ca^{2+}]_i$  transients. Because  $Ca^{2+}$ -dependent properties can influence several K<sup>+</sup> currents, and to compare with prior work, we did parallel measurements with strong  $[Ca^{2+}]_i$  buffering.

In previous studies, most K<sup>+</sup> currents were found to be downregulated in HF. In our study,  $I_{K1}$  density was indeed lower in HF under all conditions, regardless of  $[Ca^{2+}]_i$  buffering, CaMKII inhibition, or  $\beta$ -AR activation in agreement with prior work with this rabbit HF

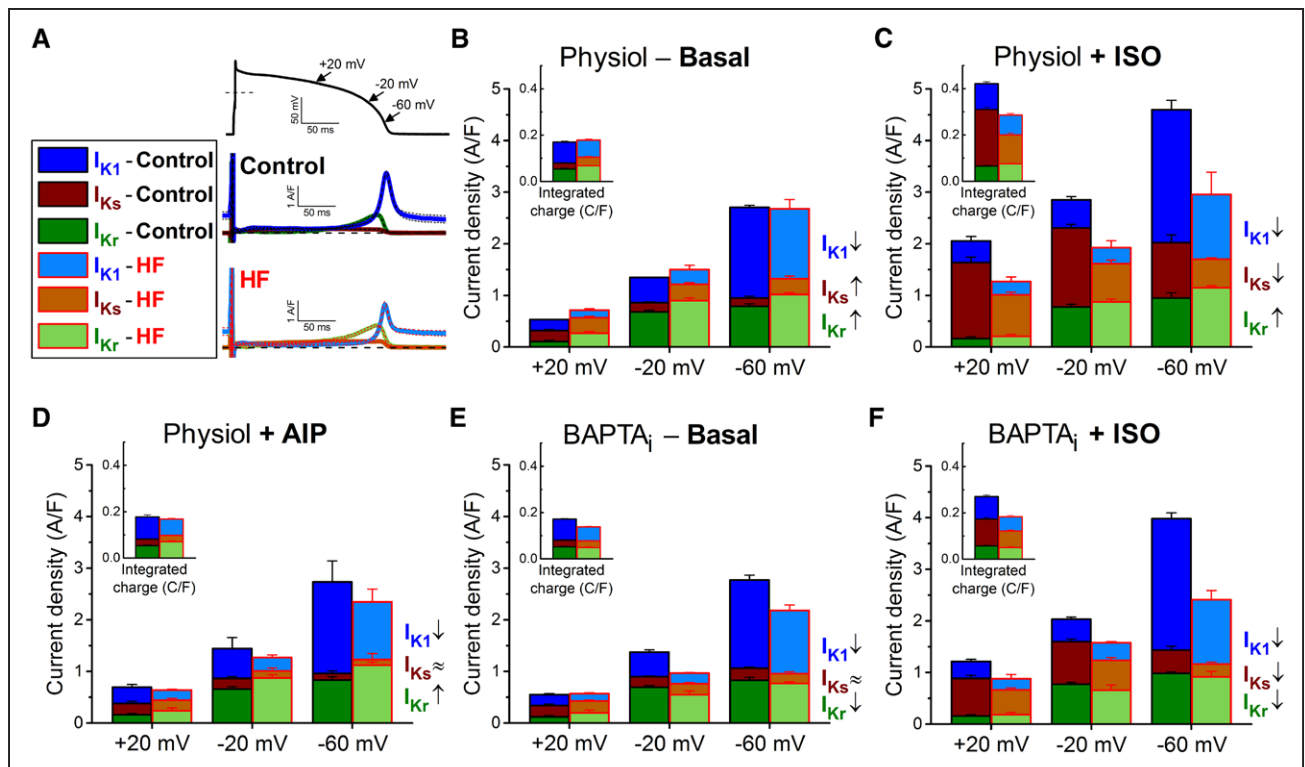


**Figure 8. Relative contribution of each K<sup>+</sup> current to net repolarizing K<sup>+</sup> current in heart failure (HF).**

Relative contributions and magnitudes of the major repolarizing K<sup>+</sup> currents ( $I_{Kr}$ ,  $I_{Ks}$ , and  $I_{K1}$ ) during action potential (AP) are compared in different phases of the repolarization process in HF to those in age-matched control. **(A)**  $I_{Kr}$ ,  $I_{Ks}$ , and  $I_{K1}$  traces in control and HF measured under AP clamp at 2 Hz without using any Ca<sup>2+</sup> buffer or  $\beta$ -AR ( $\beta$ -adrenergic receptor) agonist. Mean traces and SEM are shown. **(B)** When [Ca<sup>2+</sup>]<sub>i</sub> cycling is preserved, upregulation of  $I_{Kr}$  and  $I_{Ks}$  compensates the decrease of  $I_{K1}$  in HF during phase 3 of AP. **(C)** Stimulation of  $\beta$ -ARs using isoproterenol (ISO, 10 nmol/L) significantly upregulates  $I_{Ks}$ , thus, ISO reverses  $I_{Kr}/I_{Ks}$  dominant pattern of repolarization during phase 3 of AP. However, HF cells are hyporesponsive to ISO-induced stimulation (ie,  $I_{Ks}$  increases in a smaller extent than in control); thus, the net repolarizing current is largely reduced in HF compared with control. Reversal in  $I_{Kr}/I_{Ks}$  dominance in repolarization after ISO treatment also fail to happen in HF. **(D)** CaMKII (Ca<sup>2+</sup>/calmodulin-dependent protein kinase II) inhibition using the specific inhibitory peptide AIP (autocamtide-2-related inhibitory peptide) abolishes the increase in  $I_{Ks}$ , whereas it does not affect  $I_{Kr}$  and  $I_{K1}$ . **(E)** When [Ca<sup>2+</sup>]<sub>i</sub> is buffered (BAPTA<sub>i</sub>), the reduction in  $I_{K1}$  without the upregulation of  $I_{Kr}$  and  $I_{Ks}$  results in a significant decrease in the net repolarizing current in HF. **(F)** Under  $\beta$ -adrenergic stimulation in BAPTA<sub>i</sub>, HF cells show decrease in all 3 K<sup>+</sup> currents compared with control. The contributions of these K<sup>+</sup> currents to total net charge are shown in the insets. Columns and bars represent mean $\pm$ SEM. Statistics and *n* numbers are shown in Figures 3 through 6.

model.<sup>11</sup> However, some studies suggested that acute CaMKII inhibition could reduce  $I_{K1}$  in myocytes.<sup>19,41</sup> We cannot readily explain the differences, but one of these studies was in rabbit, using less physiological conditions, square voltage clamp pulses, and short-term cell culture to overexpress CaMKII $\delta$ .<sup>19</sup> Moreover, these studies showed that CaMKII $\delta$  overexpression in either transgenic mice or in 24 hours in rabbit myocytes induced downregulation of  $I_{K1}$  and  $K_{v}2.1$ . Because CaMKII is upregulated at the protein and activity level in HF, CaMKII-induced downregulation may explain the dominant  $I_{K1}$  downregulation that we saw in HF. Conceivably, our preincubation with the CaMKII inhibitor AIP increased channel expression to coincidentally offset an acute inhibitory effect on channel function.

Surprisingly, both  $I_{Kr}$  and  $I_{Ks}$  densities were increased during the AP in HF, under physiological AP conditions

(Figures 3 and 4). However, in both cases, this enhancement was abolished by strong [Ca<sup>2+</sup>]<sub>i</sub> buffering and for  $I_{Ks}$  by CaMKII inhibition. Ca<sup>2+</sup> sensitivity of delayed rectifier K<sup>+</sup> currents is well known, but details in the myocyte environment are still under debate.<sup>42–46</sup> For  $I_{Ks}$ , calmodulin (CaM) is an intrinsic subunit of the channel and is known to mediate Ca<sup>2+</sup>-dependent stimulation of  $I_{Ks}$  amplitude.<sup>42–44</sup> So, the BAPTA<sub>i</sub> effect to reduce  $I_{Ks}$  during the AP in HF is consistent with the myocyte Ca<sup>2+</sup> transient boosting  $I_{Ks}$  during the AP. But in control myocytes, [Ca<sup>2+</sup>]<sub>i</sub> buffering had no effect on  $I_{Kr}$  or  $I_{Ks}$  under AP clamp. The observation that CaMKII inhibition prevented the increased  $I_{Ks}$  in HF (but had no effect in control) might provide a clue explaining this apparent dichotomy. That is, if CaMKII activity (which is elevated in HF)<sup>20</sup> promotes the intrinsic Ca<sup>2+</sup> effect on  $I_{Ks}$  gating, AIP could suppress that Ca<sup>2+</sup>-dependent  $I_{Ks}$  activa-

tion. The lower CaMKII activity in control could limit that Ca<sup>2+</sup>-dependent  $I_{Ks}$  activation, explaining the lack of BAPTA, or AIP on  $I_{Ks}$  in control. In any case, basal  $I_{Ks}$  is small compared with  $I_{Kr}$  or  $I_{K1}$ , so its role in shaping the basal AP is moderate, but slightly stronger in HF.

$I_{Kr}$  upregulation was Ca<sup>2+</sup>-dependent, but CaMKII-independent.  $I_{Kr}$  is not known to be directly regulated by Ca<sup>2+</sup> or CaM, but PKC (protein kinase C) has been reported to increase  $I_{Kr}$ ,<sup>47</sup> be increased in HF,<sup>48,49</sup> and its Ca<sup>2+</sup> dependence makes this an intriguing possibility (although others found that PKC activation decreased  $I_{Kr}$  density<sup>50</sup>). Regardless of Ca<sup>2+</sup>,  $I_{Kr}$  is higher early in the AP in HF versus control, suggesting potential changes in channel gating. Possible explanations might be HF-associated alterations in subunit composition or splice variants of the channel,<sup>51</sup> and chronic  $\beta$ -AR activation (which occurs in HF) positively shifts the  $I_{Kr}$  activation voltage, independent of actual PKA activity.<sup>52</sup> Further studies are needed to elucidate the underlying molecular mechanisms for  $I_{Kr}$  and  $I_{Ks}$  upregulation in HF and the exact involvement of Ca<sup>2+</sup>, CaMKII, and PKC in their regulation.

### **$\beta$ -Adrenergic-Induced Changes in Repolarizing K<sup>+</sup> Currents in HF**

$\beta$ -AR stimulation is critical in the regulation of the heart in health and disease. Increased sympathetic activity is compensatory in early HF, but chronic  $\beta$ -AR activation also contributes to adverse remodeling in HF. On the other hand, cardiac contractile system and Ca<sup>2+</sup> handling system are hyporesponsive to  $\beta$ -AR stimulation in HF.<sup>11</sup>

$I_{Ks}$  is known to be increased by both PKA and Ca<sup>2+</sup>/CaM in ventricular myocytes<sup>44</sup> and, thus, contributes to AP shortening on  $\beta$ -AR stimulation (compensating for higher inward Ca<sup>2+</sup> and Na<sup>+</sup>/Ca<sup>2+</sup> exchange currents).<sup>27,53</sup> We found that the ISO-induced increase in  $I_{Ks}$  was suppressed in HF (both in physiological and BAPTA<sub>i</sub> conditions; Figure 6D). Indeed, the ISO effect without [Ca<sup>2+</sup>]<sub>i</sub> transients was smaller in HF, as was the increase by allowing [Ca<sup>2+</sup>]<sub>i</sub> transients in HF. The EC<sub>50</sub> ISO concentration for  $I_{Ks}$  (or  $I_{Kr}$ ) activation was not altered in HF, but the maximal effect was less than half in HF versus age-matched control (Figure 7). This may be because of the reduced number of sarcolemmal  $\beta_1$ -AR in this HF model,<sup>54</sup> and lower local cAMP levels in HF<sup>55</sup> might explain the reduced ISO response. Additionally, phosphatases and phosphodiesterases are also remodeled in HF,<sup>17</sup> which may limit  $I_{Ks}$  target phosphorylation in HF.  $I_{Kr}$  was much less affected by  $\beta$ -AR stimulation than  $I_{Ks}$  in our study and in previous reports<sup>27,53</sup> ( $\approx$ 10-fold larger change in  $I_{Ks}$  than in  $I_{Kr}$  on  $\beta$ -AR stimulation), but  $I_{Kr}$  changes are still debated. The  $\beta$ -adrenergic regulation of  $I_{Kr}$  may have species differences and involve both PKA and PKC.

$I_{Kr}$ ,  $I_{Ks}$ , and  $I_{K1}$  reach their peak density sequentially during phase 3 of AP and their relative contributions to physiological repolarization and repolarization reserve differ, as demonstrated previously in control ventricular myocytes in detail.<sup>27,56,57</sup> In this study, we demonstrated their detailed contribution to repolarization in a chronic pressure/volume overload-induced HF model (Figure 8). Important to note, that inward currents, such as late Na<sup>+</sup> current<sup>16</sup> and Na<sup>+</sup>/Ca<sup>2+</sup> exchanger current,<sup>22</sup> are also increased in HF, and  $\beta$ -AR further enhances inward Na<sup>+</sup>/Ca<sup>2+</sup> exchange and Ca<sup>2+</sup> current. These increase the demand on the repolarization reserve during phase 3 of the AP to limit APD prolongation. Therefore, any change in the delicate balance between these depolarizing and repolarizing currents in HF could have significant impact on phase 3 repolarization velocity and, thus, on APD. Accordingly, the observed Ca<sup>2+</sup>-dependent upregulation of  $I_{Kr}$  and  $I_{Ks}$  in HF may partly compensate for the loss of  $I_{K1}$  in HF and limits APD prolongation, especially at faster pacing rates when  $I_{Kr}$  may accumulate.<sup>58</sup> In line with our findings, QT<sub>c</sub> prolongation in HF patients occurs preferentially at low but not at high heart rates.<sup>15</sup> However, as we have shown in Figure 8,  $\beta$ -AR stimulation impairs the repolarization reserve capacity because of the hyporesponsive  $I_{Ks}$ .

These results also put heart rate reducing agents in HF therapy into a new perspective. The rationale of this strategy is to increase diastolic interval by which the myocardial oxygen supply/demand can be improved. Nevertheless, large clinical trials (BEAUTIFUL [Morbidity-Mortality Evaluation of the  $I_f$  Inhibitor Ivabradine in Patients With Coronary Disease and Left Ventricular Dysfunction]<sup>59</sup> and SHIFT [Systolic Heart Failure Treatment With the  $I_f$  Inhibitor Ivabradine Trial]<sup>60</sup>) found only a slight benefit of ivabradine in HF patients. Our results also suggest that  $\beta$ -AR blockers might have more benefit regarding K<sup>+</sup> currents and AP repolarization reserve and, thus, susceptibility for cardiac arrhythmias might be more reduced compared with that with heart rate-reducing agents. Another potential clinical implication is that drugs inhibiting delayed rectifier K<sup>+</sup> currents may cause even more pronounced QT<sub>c</sub> prolongation in HF patients by limiting an already diminished repolarization reserve in HF, especially during  $\beta$ -AR stimulation.

### **ACKNOWLEDGMENTS**

We thank Logan R.J. Bailey, Johanna M. Borst, Maura Ferrero, Matthew L. Stein, Ian P. Palmer, and Maximilien Bergman for their help in animal care and cell isolation.

### **SOURCES OF FUNDING**

This work was supported by grants from the National Institute of Health R01-HL30077 and P01-080101 (Dr Bers),

R01HL90880 (Drs Izu and Chen-Izu), and R01HL123526 (Dr Chen-Izu) and the American Heart Association 14GRNT20510041 (Dr Chen-Izu) and 15GRNT25860028 (Dr Pogwizd).

## DISCLOSURES

None.

## AFFILIATIONS

From the Department of Pharmacology (B.H., J.B., K.S.G., L.T.I., Y.C.-I., D.M.B.), School of Medicine, Dean's Office (L.T.), Surgical Research Facility, School of Medicine (W.T.F.), Department of Biomedical Engineering (Y.C.-I.), Department of Internal Medicine/Cardiology (Y.C.-I.), University of California, Davis; Echocardiography Laboratory, University of California, Davis Medical Center, Sacramento (L.M.M.); and Department of Medicine, University of Alabama at Birmingham (S.M.P.).

## FOOTNOTES

Received September 10, 2017; accepted December 11, 2017.

*Circ Arrhythm Electrophysiol* is available at <http://circ.ahajournals.org>.

## REFERENCES

- Tomaselli GF, Beuckelmann DJ, Calkins HG, Berger RD, Kessler PD, Lawrence JH, Kass D, Feldman AM, Marban E. Sudden cardiac death in heart failure. The role of abnormal repolarization. *Circulation*. 1994;90:2534–2539.
- Watanabe E, Arakawa T, Uchiyama T, Tong M, Yasui K, Takeuchi H, Terasawa T, Kodama I, Hishida H. Prognostic significance of circadian variability of RR and QT intervals and QT dynamicity in patients with chronic heart failure. *Heart Rhythm*. 2007;4:999–1005. doi: 10.1016/j.hrthm.2007.04.019.
- Arsenos P, Gatzoulis KA, Dilaveris P, Gialernios T, Sideris S, Lazaros G, Archontakis S, Tsiachris D, Kartsagoulis E, Stefanadis C. The rate-corrected QT interval calculated from 24-hour Holter recordings may serve as a significant arrhythmia risk stratifier in heart failure patients. *Int J Cardiol*. 2011;147:321–323. doi: 10.1016/j.ijcard.2010.12.076.
- Algra A, Tijssen JG, Roelandt JR, Pool J, Lubsen J. QTc prolongation measured by standard 12-lead electrocardiography is an independent risk factor for sudden death due to cardiac arrest. *Circulation*. 1991;83:1888–1894.
- Piccirillo G, Magri D, Matera S, Magnanti M, Torrini A, Pasquazzi E, Schifano E, Velitti S, Marigliano V, Quaglione R, Barilla F. QT variability strongly predicts sudden cardiac death in asymptomatic subjects with mild or moderate left ventricular systolic dysfunction: a prospective study. *Eur Heart J*. 2007;28:1344–1350. doi: 10.1093/eurheartj/ehl367.
- Vrtovec B, Knezevic I, Poglajen G, Sebestjen M, Okrajsek R, Haddad F. Relation of B-type natriuretic peptide level in heart failure to sudden cardiac death in patients with and without QT interval prolongation. *Am J Cardiol*. 2013;111:886–890. doi: 10.1016/j.amjcard.2012.11.041.
- Beuckelmann DJ, Näbauer M, Erdmann E. Alterations of K<sup>+</sup> currents in isolated human ventricular myocytes from patients with terminal heart failure. *Circ Res*. 1993;73:379–385.
- Li GR, Lau CP, Leung TK, Nattel S. Ionic current abnormalities associated with prolonged action potentials in cardiomyocytes from diseased human right ventricles. *Heart Rhythm*. 2004;1:460–468. doi: 10.1016/j.hrthm.2004.06.003.
- Kääb S, Nuss HB, Chiamvimonvat N, O'Rourke B, Pak PH, Kass DA, Marban E, Tomaselli GF. Ionic mechanism of action potential prolongation in ventricular myocytes from dogs with pacing-induced heart failure. *Circ Res*. 1996;78:262–273.
- Tsuji Y, Zicha S, Qi XY, Kodama I, Nattel S. Potassium channel subunit remodeling in rabbits exposed to long-term bradycardia or tachycardia: discrete arrhythmogenic consequences related to differential delayed-rectifier changes. *Circulation*. 2006;113:345–355. doi: 10.1161/CIRCULATIONAHA.105.552968.
- Pogwizd SM, Schlotthauer K, Li L, Yuan W, Bers DM. Arrhythmogenesis and contractile dysfunction in heart failure: roles of sodium-calcium exchange, inward rectifier potassium current, and residual beta-adrenergic responsiveness. *Circ Res*. 2001;88:1159–1167.
- Rose J, Aroundas AA, Tian Y, DiSilvestre D, Burysek M, Halperin V, O'Rourke B, Kass DA, Marban E, Tomaselli GF. Molecular correlates of altered expression of potassium currents in failing rabbit myocardium. *Am J Physiol Heart Circ Physiol*. 2005;288:H2077–H2087. doi: 10.1152/ajp-heart.00526.2003.
- Li GR, Lau CP, Ducharme A, Tardif JC, Nattel S. Transmural action potential and ionic current remodeling in ventricles of failing canine hearts. *Am J Physiol Heart Circ Physiol*. 2002;283:H1031–H1041. doi: 10.1152/ajp-heart.00105.2002.
- Rozanski GJ, Xu Z, Whitney RT, Murakami H, Zucker IH. Electrophysiology of rabbit ventricular myocytes following sustained rapid ventricular pacing. *J Mol Cell Cardiol*. 1997;29:721–732. doi: 10.1006/jmcc.1996.0314.
- Davey PP, Barlow C, Hart G. Prolongation of the QT interval in heart failure occurs at low but not at high heart rates. *Clin Sci (Lond)*. 2000;98:603–610.
- Valdivia CR, Chu WW, Pu J, Foell JD, Haworth RA, Wolff MR, Kamp TJ, Makielski JC. Increased late sodium current in myocytes from a canine heart failure model and from failing human heart. *J Mol Cell Cardiol*. 2005;38:475–483. doi: 10.1016/j.jmcc.2004.12.012.
- Ai X, Curran JW, Shannon TR, Bers DM, Pogwizd SM. Ca<sup>2+</sup>/calmodulin-dependent protein kinase modulates cardiac ryanodine receptor phosphorylation and sarcoplasmic reticulum Ca<sup>2+</sup> leak in heart failure. *Circ Res*. 2005;97:1314–1322. doi: 10.1161/01.RES.0000194329.41863.89.
- Wagner S, Dybkova N, Rasenack EC, Jacobshagen C, Fabritz L, Kirchhof P, Maier SK, Zhang T, Hasenfuss G, Brown JH, Bers DM, Maier LS. Ca<sup>2+</sup>/calmodulin-dependent protein kinase II regulates cardiac Na<sup>+</sup> channels. *J Clin Invest*. 2006;116:3127–3138. doi: 10.1172/JCI26620.
- Wagner S, Hacker E, Grandi E, Weber SL, Dybkova N, Sossalla S, Sowa T, Fabritz L, Kirchhof P, Bers DM, Maier LS. Ca/calmodulin kinase II differentially modulates potassium currents. *Circ Arrhythm Electrophysiol*. 2009;2:285–294. doi: 10.1161/CIRCEP.108.842799.
- Anderson ME, Brown JH, Bers DM. CaMKII in myocardial hypertrophy and heart failure. *J Mol Cell Cardiol*. 2011;51:468–473. doi: 10.1016/j.jmcc.2011.01.012.
- Hoeker GS, Hanafy MA, Oster RA, Bers DM, Pogwizd SM. Reduced arrhythmia inducibility with calcium/calmodulin-dependent protein kinase II inhibition in heart failure rabbits. *J Cardiovasc Pharmacol*. 2016;67:260–265. doi: 10.1097/FJC.0000000000000343.
- Pogwizd SM, Qi M, Yuan W, Samarel AM, Bers DM. Upregulation of Na<sup>+</sup>/Ca<sup>2+</sup> exchanger expression and function in an arrhythmogenic rabbit model of heart failure. *Circ Res*. 1999;85:1009–1019.
- Despa S, Islam MA, Weber CR, Pogwizd SM, Bers DM. Intracellular Na<sup>+</sup> concentration is elevated in heart failure but Na/K pump function is unchanged. *Circulation*. 2002;105:2543–2548.
- Zima AV, Bovo E, Bers DM, Blatter LA. Ca<sup>2+</sup> spark-dependent and -independent sarcoplasmic reticulum Ca<sup>2+</sup> leak in normal and failing rabbit ventricular myocytes. *J Physiol*. 2010;588(pt 23):4743–4757. doi: 10.1113/jphysiol.2010.197913.
- Uchinoumi H, Yang Y, Oda T, Li N, Alsina KM, Puglisi JL, Chen-Izu Y, Cornea RL, Wehrens XHT, Bers DM. CaMKII-dependent phosphorylation of RyR2 promotes targetable pathological RyR2 conformational shift. *J Mol Cell Cardiol*. 2016;98:62–72. doi: 10.1016/j.jmcc.2016.06.007.
- Banyasz T, Horvath B, Jian Z, Izu LT, Chen-Izu Y. Sequential dissection of multiple ionic currents in single cardiac myocytes under action potential-clamp. *J Mol Cell Cardiol*. 2011;50:578–581. doi: 10.1016/j.jmcc.2010.12.020.
- Banyasz T, Jian Z, Horvath B, Khabbaz S, Izu LT, Chen-Izu Y. Beta-adrenergic stimulation reverses the I<sub>Kr</sub>-I<sub>Ks</sub> dominant pattern during cardiac action potential. *Pflugers Arch*. 2014;466:2067–2076. doi: 10.1007/s00424-014-1465-7.
- Nichols CB, Chang CW, Ferrero M, Wood BM, Stein ML, Ferguson AJ, Ha D, Rigor RR, Bossuyt S, Bossuyt J. β-adrenergic signaling inhibits Gq-dependent protein kinase D activation by preventing protein kinase D translocation. *Circ Res*. 2014;114:1398–1409. doi: 10.1161/CIRCRESAHA.114.303870.

29. Banyasz T, Horvath B, Jian Z, Izu LT, Chen-Izu Y. Profile of L-type Ca(2+) current and Na(+)/Ca(2+) exchange current during cardiac action potential in ventricular myocytes. *Heart Rhythm*. 2012;9:134–142. doi: 10.1016/j.hrthm.2011.08.029.
30. Johnson DM, Heijman J, Bode EF, Greensmith DJ, van der Linde H, Abi-Gerges N, Eisner DA, Trafford AW, Volders PG. Diastolic spontaneous calcium release from the sarcoplasmic reticulum increases beat-to-beat variability of repolarization in canine ventricular myocytes after  $\beta$ -adrenergic stimulation. *Circ Res*. 2013;112:246–256. doi: 10.1161/CIRCRESA-HA.112.275735.
31. Szentandrásy N, Kistamás K, Hegyí B, Horváth B, Ruzsnavszky F, Váci K, Magyar J, Bányász T, Varró A, Nánási PP. Contribution of ion currents to beat-to-beat variability of action potential duration in canine ventricular myocytes. *Pflugers Arch*. 2015;467:1431–1443. doi: 10.1007/s00424-014-1581-4.
32. Bassani RA, Altamirano J, Puglisi JL, Bers DM. Action potential duration determines sarcoplasmic reticulum Ca<sup>2+</sup> reloading in mammalian ventricular myocytes. *J Physiol*. 2004;559(pt 2):593–609. doi: 10.1113/jphysiol.2004.067959.
33. Shannon TR, Pogwizd SM, Bers DM. Elevated sarcoplasmic reticulum Ca<sup>2+</sup> leak in intact ventricular myocytes from rabbits in heart failure. *Circ Res*. 2003;93:592–594. doi: 10.1161/01.RES.0000093399.11734.B3.
34. Curran J, Brown KH, Santiago DJ, Pogwizd S, Bers DM, Shannon TR. Spontaneous Ca waves in ventricular myocytes from failing hearts depend on Ca(2+)-calmodulin-dependent protein kinase II. *J Mol Cell Cardiol*. 2010;49:25–32. doi: 10.1016/j.yjmcc.2010.03.013.
35. Lengyel C, Iost N, Virág L, Varró A, Lathrop DA, Papp JG. Pharmacological block of the slow component of the outward delayed rectifier current (I<sub>Ks</sub>) fails to lengthen rabbit ventricular muscle QT<sub>c</sub> and action potential duration. *Br J Pharmacol*. 2001;132:101–110. doi: 10.1038/sj.bjp.0703777.
36. Zaza A, Rocchetti M, Brioschi A, Cantadori A, Ferroni A. Dynamic Ca<sup>2+</sup>-induced inward rectification of K<sup>+</sup> current during the ventricular action potential. *Circ Res*. 1998;82:947–956.
37. Straus SM, Kors JA, De Bruin ML, van der Hoof CS, Hofman A, Heeringa J, Deckers JW, Kingma JH, Sturkenboom MC, Stricker BH, Witteman JC. Prolonged QTc interval and risk of sudden cardiac death in a population of older adults. *J Am Coll Cardiol*. 2006;47:362–367. doi: 10.1016/j.jacc.2005.08.067.
38. Barr CS, Naas A, Freeman M, Lang CC, Struthers AD. QT dispersion and sudden unexpected death in chronic heart failure. *Lancet*. 1994;343:327–329.
39. Grimm M, Ling H, Willeford A, Pereira L, Gray CB, Erickson JR, Sarma S, Respress JL, Wehrens XH, Bers DM, Brown JH. CaMKII $\delta$  mediates  $\beta$ -adrenergic effects on RyR2 phosphorylation and SR Ca(2+) leak and the pathophysiological response to chronic  $\beta$ -adrenergic stimulation. *J Mol Cell Cardiol*. 2015;85:282–291. doi: 10.1016/j.yjmcc.2015.06.007.
40. Kääb S, Dixon J, Duc J, Ashen D, Näbauer M, Beuckelmann DJ, Steinbeck G, McKinnon D, Tomaselli GF. Molecular basis of transient outward potassium current downregulation in human heart failure: a decrease in Kv4.3 mRNA correlates with a reduction in current density. *Circulation*. 1998;98:1383–1393.
41. Nagy N, Acsai K, Kormos A, Sebök Z, Farkas AS, Jost N, Nánási PP, Papp JG, Varró A, Tóth A. [Ca<sup>2+</sup>]<sub>i</sub>-induced augmentation of the inward rectifier potassium current (I<sub>K1</sub>) in canine and human ventricular myocardium. *Pflugers Arch*. 2013;465:1621–1635. doi: 10.1007/s00424-013-1309-x.
42. Tohse N. Calcium-sensitive delayed rectifier potassium current in guinea pig ventricular cells. *Am J Physiol*. 1990;258(4 pt 2):H1200–H1207. doi: 10.1152/ajpheart.1990.258.4.H1200.
43. Xie Y, Ding WG, Matsuura H. Ca<sup>2+</sup>/calmodulin potentiates I<sub>Ks</sub> in sinoatrial node cells by activating Ca<sup>2+</sup>/calmodulin-dependent protein kinase II. *Pflugers Arch*. 2015;467:241–251. doi: 10.1007/s00424-014-1507-1.
44. Bartos DC, Morotti S, Ginsburg KS, Grandi E, Bers DM. Quantitative analysis of the Ca<sup>2+</sup>-dependent regulation of delayed rectifier K<sup>+</sup> current I<sub>Ks</sub> in rabbit ventricular myocytes. *J Physiol*. 2017;595:2253–2268. doi: 10.1113/JP273676.
45. Nitta J, Furukawa T, Marumo F, Sawanobori T, Hiraoka M. Subcellular mechanism for Ca(2+)-dependent enhancement of delayed rectifier K<sup>+</sup> current in isolated membrane patches of guinea pig ventricular myocytes. *Circ Res*. 1994;74:96–104.
46. Ghosh S, Nunziato DA, Pitt GS. KCNQ1 assembly and function is blocked by long-QT syndrome mutations that disrupt interaction with calmodulin. *Circ Res*. 2006;98:1048–1054. doi: 10.1161/01.RES.0000218863.44140.f2.
47. Heath BM, Terrar DA. Protein kinase C enhances the rapidly activating delayed rectifier potassium current, I<sub>Kr</sub>, through a reduction in C-type inactivation in guinea-pig ventricular myocytes. *J Physiol*. 2000;522(pt 3):391–402.
48. Bowling N, Walsh RA, Song G, Estridge T, Sandusky GE, Fouts RL, Mintze K, Pickard T, Roden R, Bristow MR, Sabbah HN, Mizrahi JL, Gromo G, King GL, Vlahos CJ. Increased protein kinase C activity and expression of Ca<sup>2+</sup>-sensitive isoforms in the failing human heart. *Circulation*. 1999;99:384–391.
49. Braz JC, Gregory K, Pathak A, Zhao W, Sahin B, Kleivitsky R, Kimball TF, Lorenz JN, Nairn AC, Liggett SB, Bodi I, Wang S, Schwartz A, Lakatta EG, DePaoli-Roach AA, Robbins J, Hewett TE, Bibb JA, Westfall MV, Kranias EG, Molkenin JD. PKC- $\alpha$  regulates cardiac contractility and propensity toward heart failure. *Nat Med*. 2004;10:248–254. doi: 10.1038/nm1000.
50. Cockerill SL, Tobin AB, Torrecilla I, Willars GB, Standen NB, Mitcheson JS. Modulation of hERG potassium currents in HEK-293 cells by protein kinase C. Evidence for direct phosphorylation of pore forming subunits. *J Physiol*. 2007;581(pt 2):479–493. doi: 10.1113/jphysiol.2006.123414.
51. Holzem KM, Gomez JF, Glukhov AV, Madden EJ, Koppel AC, Ewald GA, Trenor B, Efimov IR. Reduced response to I<sub>Kr</sub> blockade and altered hERG1a/1b stoichiometry in human heart failure. *J Mol Cell Cardiol*. 2016;96:82–92. doi: 10.1016/j.yjmcc.2015.06.008.
52. Shu L, Zhang W, Su G, Zhang J, Liu C, Xu J. Modulation of hERG K<sup>+</sup> channels by chronic exposure to activators and inhibitors of PKA and PKC: actions independent of PKA and PKC phosphorylation. *Cell Physiol Biochem*. 2013;32:1830–1844. doi: 10.1159/000356616.
53. Szentandrásy N, Farkas V, Bárándi L, Hegyí B, Ruzsnavszky F, Horváth B, Bányász T, Magyar J, Márton I, Nánási PP. Role of action potential configuration and the contribution of Ca<sup>2+</sup> and K<sup>+</sup> currents to isoprenaline-induced changes in canine ventricular cells. *Br J Pharmacol*. 2012;167:599–611. doi: 10.1111/j.1476-5381.2012.02015.x.
54. Desantiago J, Ai X, Islam M, Acuna G, Ziolo MT, Bers DM, Pogwizd SM. Arrhythmogenic effects of beta2-adrenergic stimulation in the failing heart are attributable to enhanced sarcoplasmic reticulum Ca load. *Circ Res*. 2008;102:1389–1397. doi: 10.1161/CIRCRESAHA.107.169011.
55. Barbargallo F, Xu B, Reddy GR, West T, Wang Q, Fu Q, Li M, Shi Q, Ginsburg KS, Ferrier W, Isidori AM, Naro F, Patel HH, Bossuyt J, Bers D, Xiang YK. Genetically encoded biosensors reveal PKA hyperphosphorylation on the myofilaments in rabbit heart failure. *Circ Res*. 2016;119:931–943. doi: 10.1161/CIRCRESAHA.116.308964.
56. Bányász T, Magyar J, Szentandrásy N, Horváth B, Birinyi P, Szentmiklósi J, Nánási PP. Action potential clamp fingerprints of K<sup>+</sup> currents in canine cardiomyocytes: their role in ventricular repolarization. *Acta Physiol (Oxf)*. 2007;190:189–198. doi: 10.1111/j.1748-1716.2007.01674.x.
57. Jost N, Virág L, Bitay M, Takács J, Lengyel C, Biliczki P, Nagy Z, Bogáts G, Lathrop DA, Papp JG, Varró A. Restricting excessive cardiac action potential and QT prolongation: a vital role for I<sub>Ks</sub> in human ventricular muscle. *Circulation*. 2005;112:1392–1399. doi: 10.1161/CIRCULATIONAHA.105.550111.
58. Jurkiewicz NK, Sanguinetti MC. Rate-dependent prolongation of cardiac action potentials by a methanesulfonanilide class III antiarrhythmic agent. Specific block of rapidly activating delayed rectifier K<sup>+</sup> current by dofetilide. *Circ Res*. 1993;72:75–83.
59. Fox K, Ford I, Steg PG, Tendera M, Ferrari R; BEAUTIFUL Investigators. Ivabradine for patients with stable coronary artery disease and left ventricular systolic dysfunction (BEAUTIFUL): a randomised, double-blind, placebo-controlled trial. *Lancet*. 2008;372:807–816. doi: 10.1016/S0140-6736(08)61170-8.
60. Swedberg K, Komajda M, Böhm M, Borer JS, Ford I, Dubost-Brama A, Lerebourg G, Tavazzi L; SHIFT Investigators. Ivabradine and outcomes in chronic heart failure (SHIFT): a randomised placebo-controlled study. *Lancet*. 2010;376:875–885. doi: 10.1016/S0140-6736(10)61198-1.